Canadian Technical Report of
Hydrography and Ocean Sciences 208

2000

Sea Ice Fluctuations in the Western Labrador Sea (1963-1998)

by

I.K. Peterson, S.J. Prinsenberg and P. Langille

Ocean Sciences Division
Maritimes Region
Fisheries and Oceans Canada

Bedford Institute of Oceanography
P.O. Box 1006
Dartmouth, Nova Scotia
Canada, B2Y 4A2

Cat. No. Fs97-18/208 E ISSN:0711-6764

Correct Citation for this publication:

Peterson, I.K., S.J. Prinsenberg and P. Langille. 2000. Sea Ice Fluctuations in the Western Labrador Sea (1963-1998). Can. Tech. Rep. Hydrogr. Ocean Sci. 208: v + 51 p.

TABLE OF CONTENTS

ABSTRACT

Peterson, I.K., S.J. Prinsenberg and P. Langille. 2000. Sea Ice Fluctuations in the Western Labrador Sea (1963-1998). Can. Tech. Rep. Hydrogr. Ocean Sci. 208: v + 51 p.

This atlas describes sea ice fluctuations in the western Labrador Sea during 1963 to 1998 inclusive. The data set consists of ice concentrations on a 0.5° latitude by 1.0° longitude grid, derived from weekly ice charts published by the Canadian Ice Service. The data set was compiled from several sources, each covering different periods. The ice charts were digitized between 45° and 65°N with respect to total ice concentration, and the concentration of individual ice types (new, grey, grey-white, first-year and old). Monthly maps showing median, minimum and maximum ice concentrations and the median proportion of first year ice (>30 cm) are presented. Time series of sea ice extent, ice extent anomalies, icebergs south of 48°N, air temperature and surface wind, and results of regression analysis are also included. The annual number of icebergs drifting south of 48°N is most strongly correlated with sea ice extent off Newfoundland between 47 and 52°N from April to June. Because of the high persistence of sea ice, the best predictor of both spring sea ice extent (Apr-Jun) and iceberg numbers south of 48°N is sea ice extent several months earlier.

RÉSUMÉ

Peterson, I.K., S.J. Prinsenberg and P. Langille. 2000. Sea Ice Fluctuations in the Western Labrador Sea (1963-1998). Can. Tech. Rep. Hydrogr. Ocean Sci. 208: v + 51 p.

Le présent atlas décrit les fluctuations des glaces marines dans l'ouest de la mer du Labrador de 1963 à 1998. L'ensemble de données porte notamment sur les concentrations de glace dans une grille de 0,5 ^{o} de latitude et 1,0 ^{o} de longitude, d'après les cartes hebdomadaires des glaces publiées par le Service canadien des glaces. Cet ensemble de données a été établi à partir de plusieurs sources, couvrant des périodes différentes. Les cartes des glaces ont été numérisées entre 45 ^{o} et 65 ^{o} N pour ce qui concerne la concentration totale de glaces et la concentration des types de glace (glace nouvelle, glace grise, glace blanchâtre, glace de l'année, vieille glace). Des cartes mensuelles illustrant les concentrations médianes, minimales et maximales des glaces ainsi que la proportion médiane de glace de l'année (>30 cm) sont présentées. L'ensemble comprend également des séries chronologiques sur l'étendue des glaces marines, sur les anomalies de cette étendue, sur les icebergs au sud de 48 ^{o} N, sur la température de l'air et sur les vents de surface, ainsi que les résultats d'analyses de régression. Il existe une forte corrélation entre le nombre annuel d'icebergs qui dérivent au sud de 48 ^{o} N et l'étendue des glaces marines au large de Terre-Neuve, entre 47 et 52 ^{o} N, d'avril à juin. En raison de la forte persistance des glaces marines, le meilleur facteur de prévision à la fois de l'étendue des glaces marines au printemps (avril-juin) et du nombre d'icebergs au sud de 48 ^{o} N est l'étendue des glaces marines plusieurs mois auparavant.

1 Introduction

Sea ice off Labrador and Newfoundland poses a major hazard for shipping and for offshore hydrocarbon exploration and development. Ice conditions in the Labrador Sea region have been described in several atlases. Some concentrate on describing mean ice conditions for each week of the year, while others describe the interannual variability of ice concentration or extent in the form of time series. For example, charts showing the probability of ice within 0.5° latitude by 1.0° longitude squares for each week of the year are presented for the Southern Labrador/Newfoundland region in Markham (1980), and for the Davis Strait/Labrador region in Markham (1988). In addition, Markham (1980) describes seasonal changes of ice type, i.e. the stages of development of ice. Charts of the median, minimum and maximum position of the ice edge for each week of the year are presented for the region south of Davis Strait in Sowden and Geddes (1980), and for the Southern Labrador/Newfoundland region in Cote (1989). These atlases show the climatological mean ice conditions, as well as a general measure of the interannual variability. On the other hand, Manak and Mysak (1987) have described the interannual variability from 1953 to 1984 for the entire Arctic region by presenting seasonal maps of ice concentration, and time series of ice extext anomalies based on monthly ice concentration data on a 1° latitude by 1° longitude grid.

The interannual variability of sea ice conditions for the western Labrador Sea was described for the years 1963 to 1988 in Peterson and Prinsenberg (1990), based on ice charts from the Canadian Ice Service which were digitized on a 0.5° latitude by 1° longitude grid. This report provides an update covering the years up to 1998. The sea ice data are compared with air temperature, surface wind and icebergs over the same period.

2 Description of data set

Composite ice charts are produced at the Canadian Ice Service for several regions from 1 to 3 times per week during the operational season, and at least once per month at other times (Atmospheric Environment Service, 1992). The charts provide concentrations and floe sizes for the various ice types representing different thicknesses. The ice types refer to level, undeformed ice, not ice deformed by rafting and ridging. The charts are based on (a) satellite sources (NOAA AVHRR, LANDSAT, SSM/I, SPOT, RADARSAT and ERS), (b) aircraft sources (SLAR and SAR, visual observations of ice type and concentration, ice thickness measurements from helicopter reconnaissance flights), (c) vessel sources (visual observations of ice type and thickness), (d) shore station sources (visual observations and ice thickness measurements), and (e) other sources (drifting beacons, freezing-degree days).

Ice charts for the Canadian east coast were digitized to provide concentrations of the various ice types on a 0.5° latitude by 1° longitude grid by the following:
1) 1963-1972 W. E. Markham (Ice Centre, AES)
2) 1973-1978 Esso Resources

The data set described in this report was compiled from these two sources for the years 1963-1978. For subsequent years, weekly composite ice charts for the Eastern Coast region (south of 56°N) and Hudson Bay and Approaches (north of 55°N) were obtained from the Canadian Ice Service and were then digitized by:
1) 1978-1985 Martec Ltd.
2) 1986-1988 45-56°N: Martec Ltd.
3) 1986-1988 56-65°N: M. Murphy, Canadian Seabed Research
4) 1989-1998 P. Langille

The data set consists of the weekly total concentration of ice in each 0.5° latitude by 1° longitude grid square for the area shown in Fig. 2.1, as well as the concentration of each of the following constituents:
1) New Ice (0-10 cm)
2) Grey Ice (10-15 cm)
3) Grey-White Ice (15-30 cm)
4) First-Year Ice (>30 cm)
5) Old Ice (ice which has survived at least one melt season)

Since 1982, more thickness categories have been shown on the ice charts, but are not included in the digitized data set.

Some data are missing for the following reasons:
1) There is a lack of satellite observations for the early years, so that total areal coverage is reduced.
2) Sometimes, the areal coverage of ice is known, but not the concentration.
3) Sometimes, the total concentration is known, but not the concentration of individual ice types.
4) For the region of Hudson Bay and Approaches, charts are available only for the first of the month for January to April after 1978. For this reason and because of limited text space, this atlas displays maps for the date closest to the first of each month, even though the data set consists of weekly digitized data for most areas and times.

Other data sets used in this report are:

(a) Number of icebergs drifting south of 48°N: from the International Ice Patrol (IIP) (Anderson, 1993).

(b) Air temperature at Iqaluit, N.W.T, Cartwright, Labrador and St. John's, Newfoundland.

(c) Surface Winds (.995 sigma level): NCEP Reanalysis data provided by the NOAA-CIRES Climate Diagnostics Center, Boulder, Colorado, from their Web site at http://www.cdc.noaa.gov/.

(d) North Atlantic Oscillation (NAO) Index: winter (December, January, February) sea level pressure difference between Ponta Delgada, Azores and Akureyri, Iceland (Drinkwater, 1995)

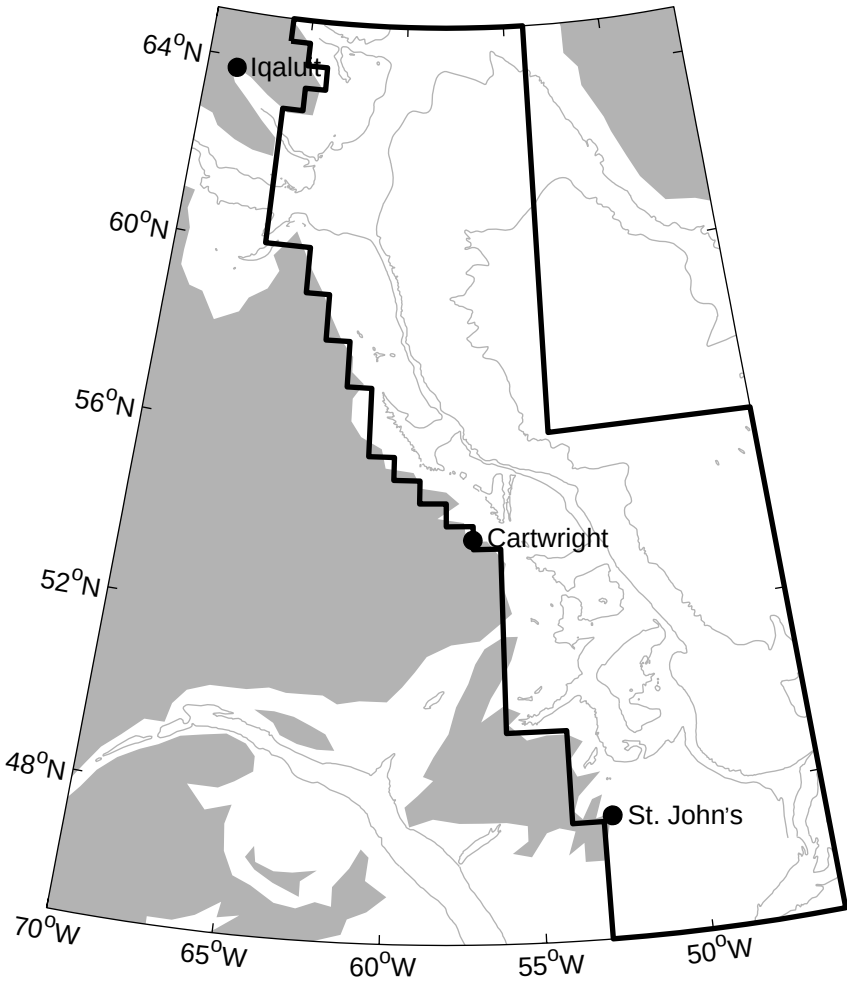

Fig. 2.1. The western Labrador Sea region, showing the area described in this report (heavy line). The 300, 1000 and 3000 m bottom contours are also shown.

3 Sea ice concentration and extent

Median ice concentrations (1963-1998) at the start of each month in each grid cell are shown in Appendix A (upper left). These plots may underestimate the expected southern limit, since grid cells having less than half of their total area within the ice edge are excluded from the digital database. The median fraction of ice thicker than 30 cm at the start of each month in each grid cell is shown in the upper right corner. Also shown are the minimum ice concentration (lower left) and the maximum concentration (lower right).

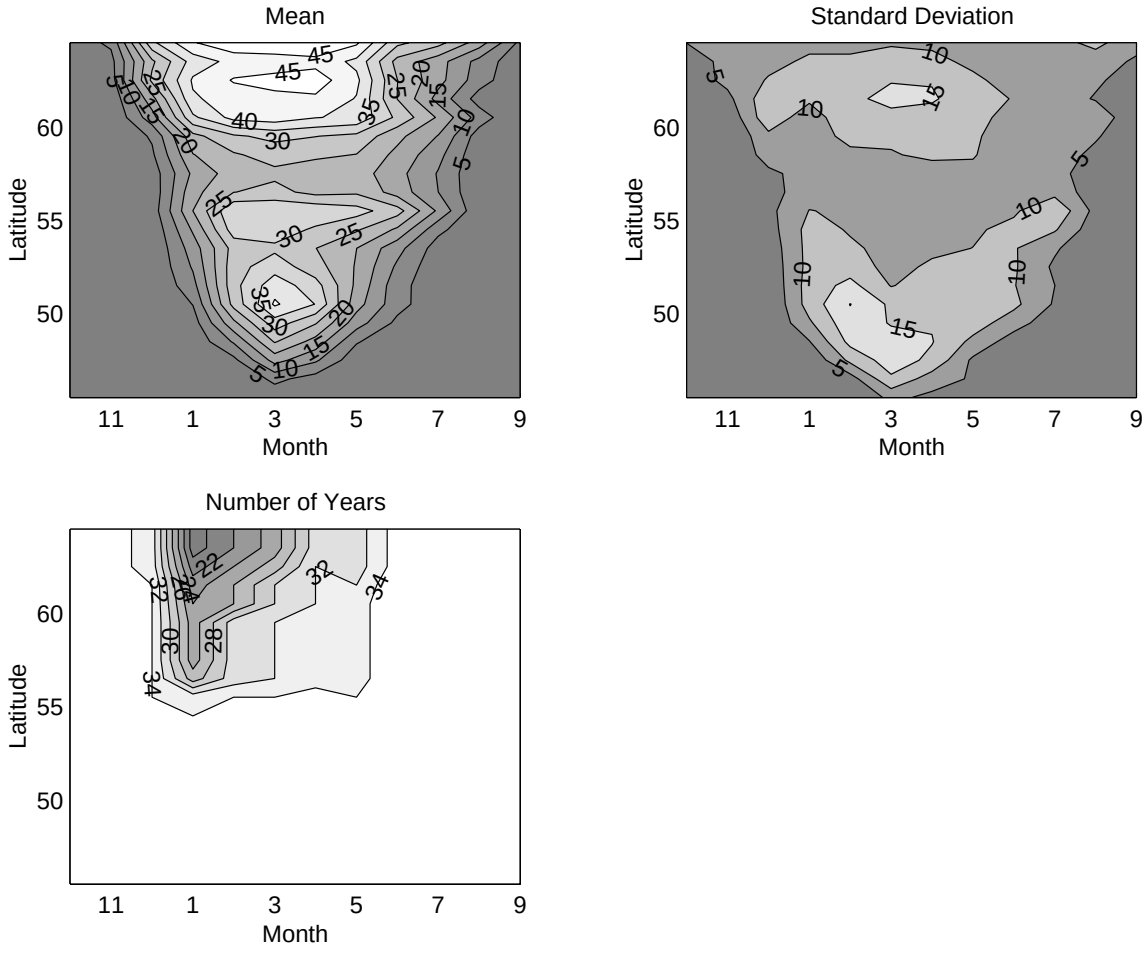

Fig. 3.1. Mean, standard deviation of sea ice extent ($km^2 *10^3$ / (° latitude)) and number of years of data in the western Labrador Sea at the start of each month in each latitude band.

The mean ice extent, or area inside the ice edge, was computed for each band of latitude at the start of each month (Fig. 3.1). The resolution of ice extent is 0.5° latitude by 1.0° longitude. North of 50°N, the spatial pattern reflects changes in the width of the shelf. The mean ice extent decreases south of 60°N where the 3000 m isobath moves shoreward, and increases at 55°N and south of

52°N where the shelf widens; this is also seen in maps of median ice concentration (Appendix A). Temporally, the ice extent remains high in the north from February to April. At 55°N, the maximum ice extent is in February, while to the south at 50°N, the maximum is in March.

The standard deviation is high east of Hudson Strait at 62°N and in the Northeast Newfoundland Shelf/Grand Banks region at 47-51°N (Fig. 3.1). This is reflected in maps of the minimum and maximum ice concentration (Appendix A). The standard deviation of ice extent is low from 56-58°N because the distance between the 100 and 3000 m isobaths is narrower in this region than to the north or south. In general, the 100 and 3000 m isobaths define the minimum and maximum limits of the February-May ice edge. South of 52°N, the standard deviation of ice extent is also high because of variability in the southern limit of the ice edge.

The number of years of data is lowest north of 55°N, especially in January-March (Fig. 3.1). The missing data are generally in the 1960's and 1970's. Since the shipping routes between North American and European ports cross the analysis area south of 55°N, data collection and chart production are concentrated on the southern region during the winter months.

Time series of sea ice extent at the start of each month in each latitude band are shown in Fig. 3.2, with the monthly anomalies plotted in Fig. 3.3. North of 60°N, anomalies are high in 1972-1973, 1983-1984, 1990 and 1993. At 50°N, anomalies are high in 1972-1974, 1983-1985, and 1990-1994. Although there is some suggestion of a 1-2 year lag of ice in the south behind ice in the north, this may simply reflect trends in meteorological patterns.

Correlations of ice extent south of 55°N between different months are shown in Table 3.1. The persistence from January to February is high (r=0.85). From April to June, the correlations are no higher with ice extent in the previous month than with February ice extent.

Table 3.1. Correlation coefficients (r) of ice extent south of 55°N between different months, 1963-1998.

	Feb	**Mar**	**Apr**	**May**	**Jun**	**Jul**
Jan	0.85	0.48	0.49	0.64	0.44	0.21
Feb		0.65	0.55	0.68	0.62	0.38
Mar			0.54	0.42	0.63	0.47
Apr				0.49	0.29	0.26
May					0.57	0.51
Jun						0.81

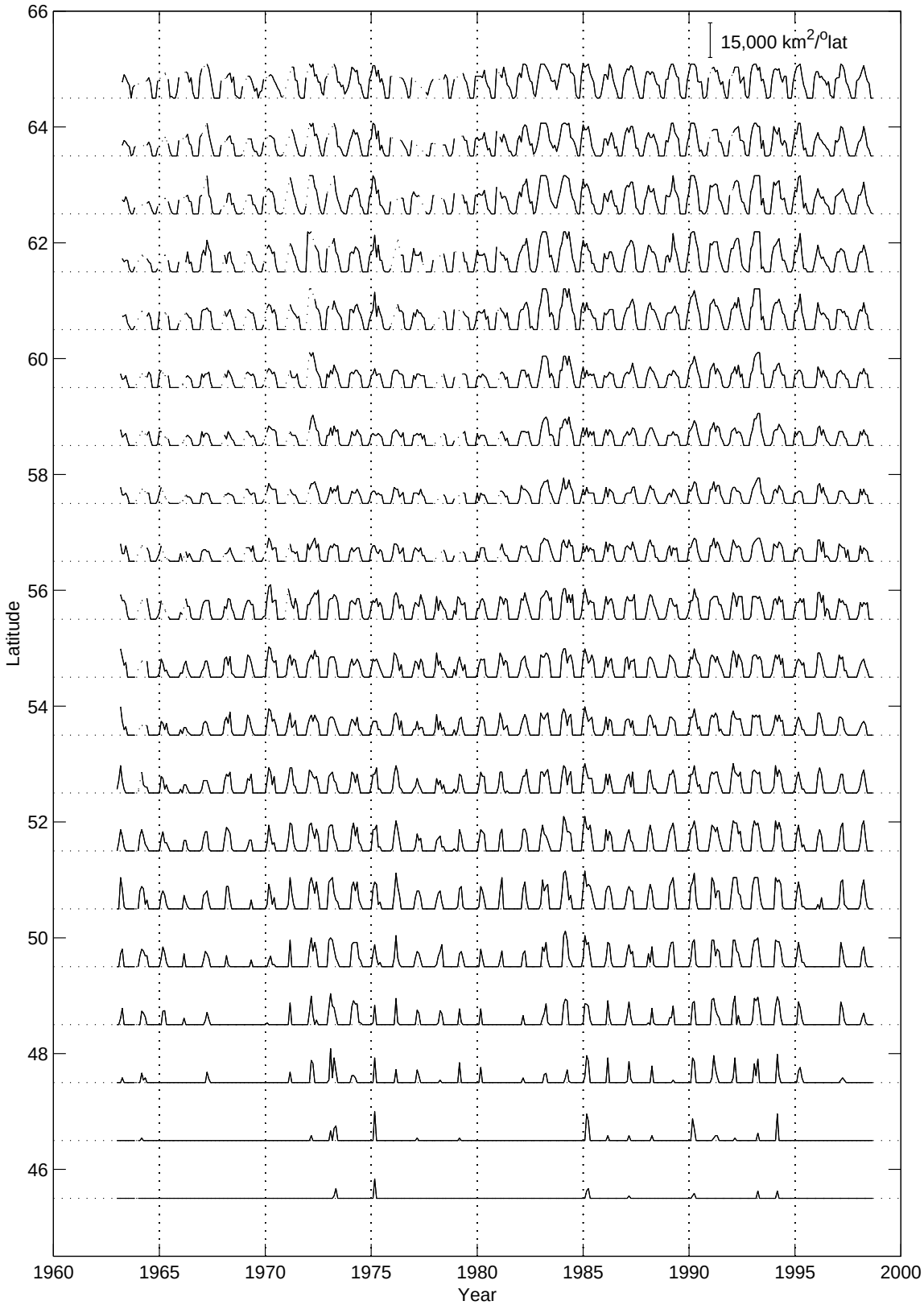

Fig. 3.2. Time series of sea ice extent ($km^2 * 10^3$ / (° latitude)) in the western Labrador Sea at the start of each month in each latitude band.

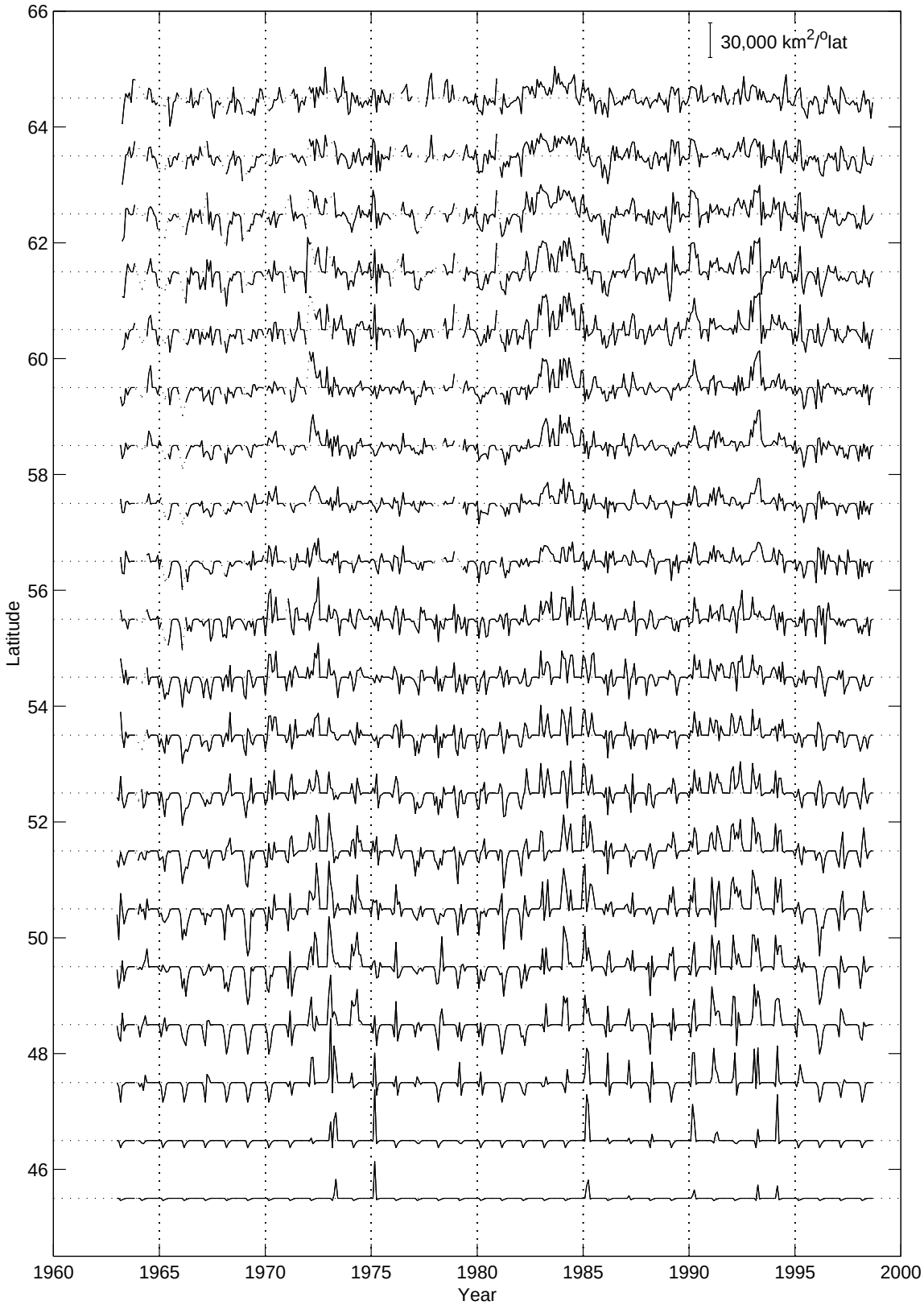

Fig. 3.3. Time series of anomalies of sea ice extent ($km^2 *10^3$ / (° latitude)) in the western Labrador Sea at the start of each month in each latitude band.

4 Icebergs

The prediction of annual iceberg numbers off Newfoundland has been studied since the early 1900's, and is important for the planning of safe shipping routes. It has long been known that there is a strong relationship between the number of icebergs and annual fluctuations in Newfoundland sea ice extent. Smith (1931) found a correlation coefficient of 0.86 between annual iceberg numbers south of Newfoundland (most of which are observed from mid-March to mid-June) and sea ice extent from February to May for the period 1880-1926. The high correlation is probably due to the role of sea ice in reducing the rate of iceberg deterioration. Sea ice protects icebergs in the following ways: (1) waves are quickly damped at the edge of the pack, (2) the water temperature is maintained near the freezing point, and (3) icebergs are prevented from grounding in fjords and embayments (Robe, 1980).

High correlations between sea ice extent and icebergs are also found using more recent sea ice extent data both off Newfoundland (south of 55°N) on April 15 and to the north in Davis Strait (61-67°N, 50-64°W) in January; sea ice extent in the two regions are highly correlated (Marko et al., 1994). In this section, the spatial-temporal relationship between icebergs and sea ice are examined in more detail.

The traditional measure of annual iceberg severity is the number of icebergs drifting south of latitude 48°N, estimated by the International Ice Patrol (Anderson, 1993). It is based on iceberg sightings and on modeling of the icebergs' drift and deterioration. The modeling is necessary to correct for resightings of the same iceberg, and to determine whether an iceberg sighted north of 48°N deteriorates before crossing 48°N. The estimate is highly subjective and is affected by numerous changes in technology and methodology over the years. The number of icebergs south of 48°N are plotted in Fig. 4.1 for the period 1959-1998. The number is high in 1972-1974, 1983-1985, 1991-1995 and 1997-1998, similar to the years in which ice extent was high south of 50°N (Fig. 3.2).

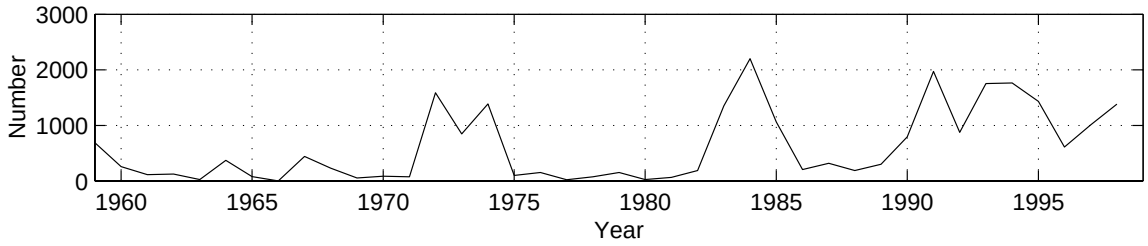

Fig. 4.1. Time series of the annual number of icebergs south of 48°N, 1959-1998.

Correlations between iceberg numbers and ice extent in each latitude band at the start of each month are shown in Fig. 4.2. In general they reflect the

spatial pattern observed for the standard deviation of ice extent (Fig. 3.1). In January, the correlations are greater than 0.6 at 60°N and 51-56°N, while in February, they are high at 58-61°N and 48-51°N.

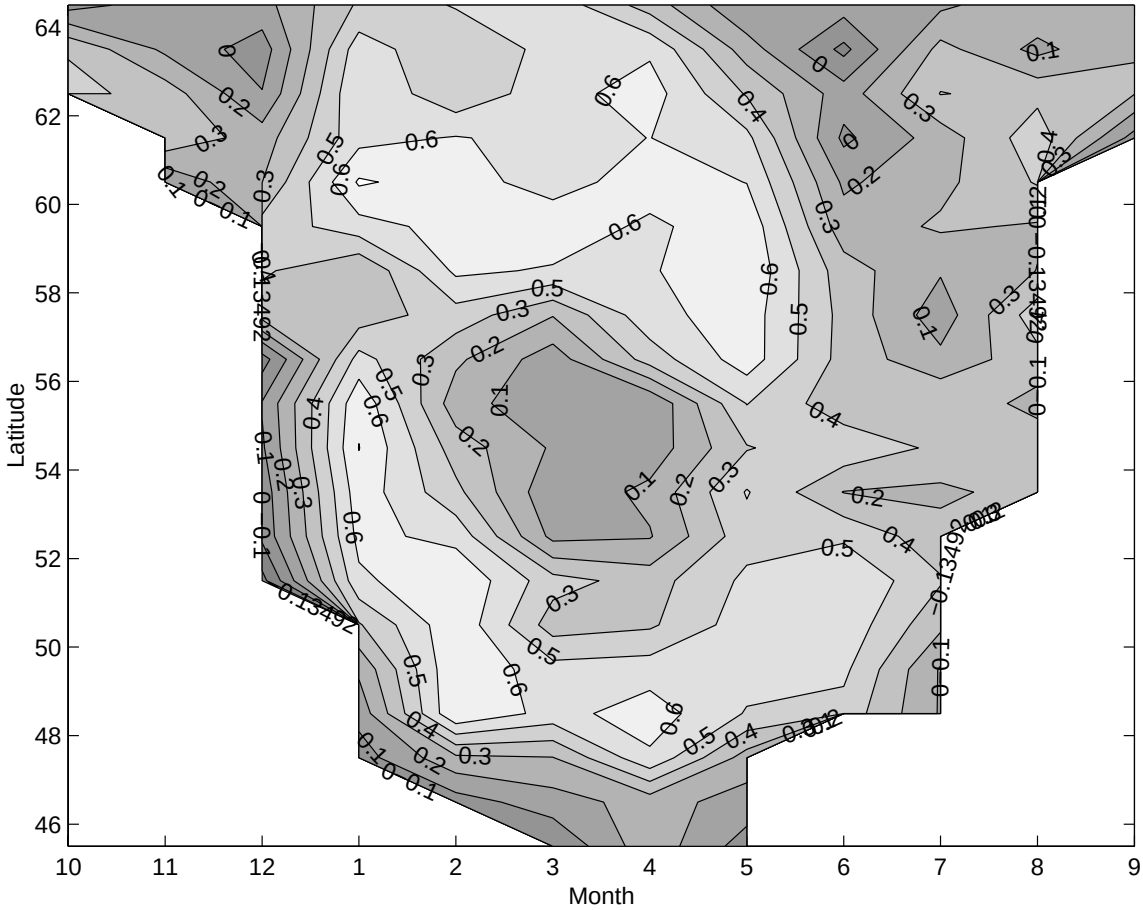

Fig. 4.2. Correlation coefficients (r) between annual iceberg numbers south of 48°N and sea ice extent in the western Labrador Sea at the start of each month in each latitude band.

For the region south of 55°N, the latitude ranges of sea ice extent in each month giving the highest correlation with annual iceberg number are listed at the top of Table 4.1. These particular ranges have the highest correlations, since they correspond to the position of the southern ice edge where the variance of ice extent is highest. The monthly values of sea ice extent were then averaged over different month ranges. The highest overall correlation is with sea ice extent from April 1 to June 1 (r=0.82), the period when the number of icebergs drifting south of 48°N is highest. For February-June, the period used by Smith (1931), the correlation is only slightly lower (r=0.80). For the total ice extent south of 55°N, the correlation is maximal for the period April-June (r=0.77). Differences

between these three correlation coefficients are probably not statistically significant.

Table 4.1. Correlation coefficients (r) between annual iceberg numbers south of 48°N and sea ice extent averaged over latitude bands and months, 1963-1998.

		Last Month of Sea Ice Extent Averaging						
First Month of Sea Ice Extent Averaging		Jan 54-55°N	Feb 48-52°N	Mar 48-50°N	Apr 47-49°N	May 47-52°N	Jun 48-52°N	Jul 48-53°N
	Jan	**0.70**	**0.73**	**0.73**	**0.78**	**0.79**	0.80	0.80
	Feb		0.72	0.72	0.77	0.79	0.80	0.80
	Mar			0.57	0.73	0.77	0.80	0.80
	Apr				0.67	0.73	**0.82**	**0.81**
	May					0.67	0.72	0.70
	Jun						0.61	0.58
	Jul							0.42

It can be seen that the correlation between time-averaged sea ice extent and annual iceberg numbers increases over time from 0.70 for January ice extent to 0.82 for April to June ice extent. Thus half the variance of iceberg numbers can be explained by January, and two-thirds by June using the April-June ice extent.

In January, the correlation of iceberg numbers with sea ice extent is also high to the north at 60-61°N (r=0.71, Fig. 4.1), though fewer data are available for the northern latitudes. Marko et al. (1994) also observed a high correlation with maximum ice extent throughout the month of January in Davis Strait (61-67°N), and suggested that it may determine spring ice extent off Newfoundland. However, it appears from this study that correlations are also high over much of the area to the south down to 51°N near the southern ice limit for January, and are not confined to Davis Strait. A combination of ice extent at 60-61°N and at 54-55°N does not significantly improve the correlation with icebergs.

The iceberg time series is plotted in Fig. 4.3, along with the numbers estimated from sea ice extent for 48-52°N (Apr-Jun) and 54-55°N in January using the following regression equations:

$N = 72.25 * E_1 \quad - 80.20 \quad (r^2 = 0.67)$

$N = 40.41 * E_2 \quad + 33.89 \quad (r^2 = 0.49)$

where N = Iceberg numbers south of 48°N
E_1 = Sea ice extent 47-52°N (Apr-Jun)
E_2 = Sea ice extent 54-55°N (Jan)

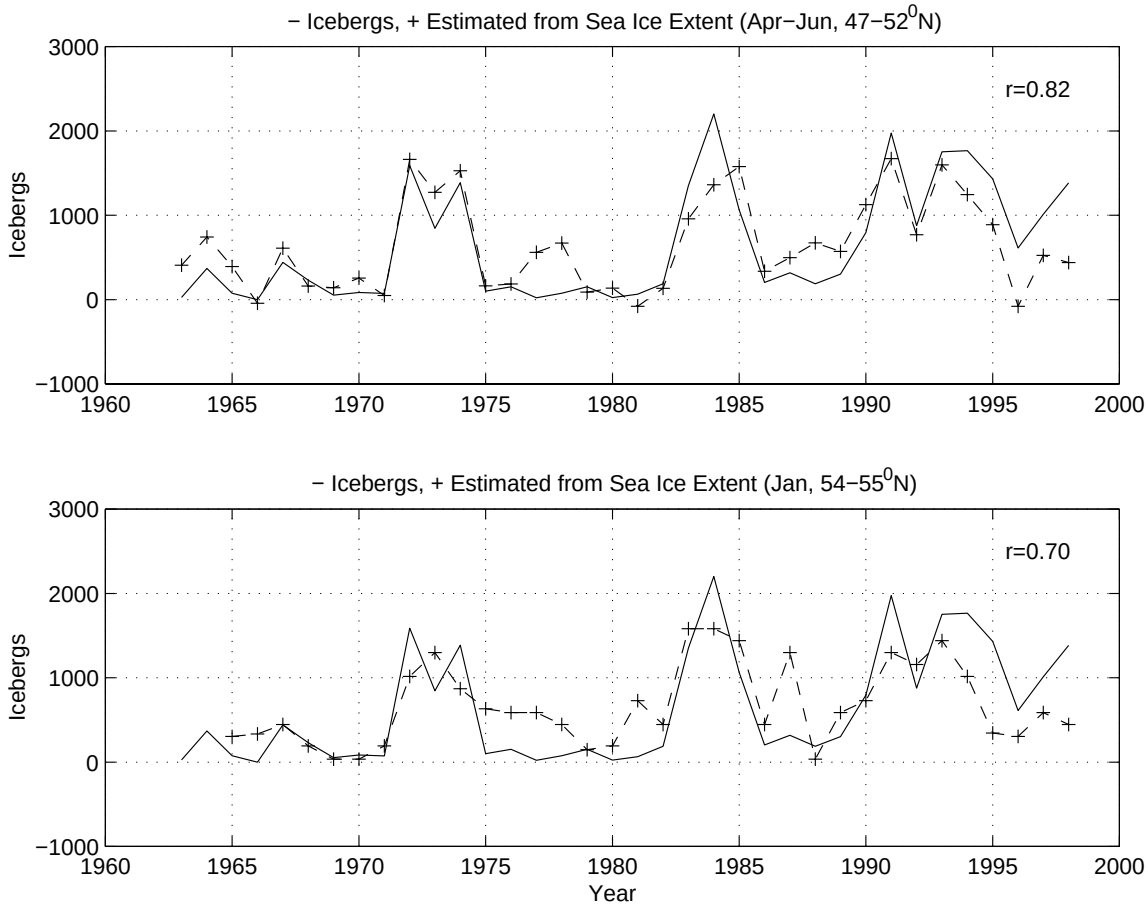

Fig. 4.3. Time series of the number of icebergs south of 48°N, and numbers estimated from ice extent (47-52°N, Apr-Jun), and (54-55°N, Jan).

5 Air Temperature

Winter and spring sea ice extent south of 55°N are highly correlated with negative air temperature at Cartwright and St. John's (Prinsenberg et al., 1997). In this section, correlations between air temperature and sea ice extent are presented for various time lags, and over an area extending further north.

Correlations between monthly negative air temperature at Iqaluit, Cartwright and St. John's with sea ice at the start of each month in each latitude band are shown in Appendix B. A correlation of 0.33 is significant at the 95% level for 36 independent observations. The number of independent observations is generally less than 36 due to autocorrelation, and to missing data in the north.

For Iqaluit, the highest correlations are between negative air temperature in December to February and sea ice 0-4 months later north of 55°N. Negative air temperatures from March to May are correlated to a lesser degree with ice 0-1 month later. Correlations from June to November are generally low.

A similar pattern is present for Cartwright. The highest correlations are between negative air temperature in December to February and sea ice 0-2 months later north of 48°N. North of 58°N, they are generally lower than for Iqaluit. Negative air temperatures from March to May are most highly correlated with ice 1-2 months later, but correlations are lower than for winter negative air temperatures. Correlations from June to November are generally low.

For St. John's, the correlations are for the most part lower than for Cartwright, except for negative air temperatures in February and March which are more highly correlated with ice south of 48°N 0-1 month later.

In general, the results are consistent with those of Walsh and Johnson (1979) showing that for the Arctic as a whole, ice extent during the months of ice growth (Oct-Jan) is most highly correlated with atmospheric data over the preceding 1-2 months. During ice retreat (Feb-Jul), correlations are highest with the previous 5 months of atmospheric data.

Newfoundland sea ice extent from 47 to 52°N (Apr-Jun), which is most highly correlated with icebergs, was compared with air temperature at Iqaluit, Cartwright and St. John's averaged over periods of 1 to 8 months between October and May. The correlations for the winter period (Dec-Feb) are shown in Table 5.1. Correlations are also shown for ice extent south of 55°N (Apr-Jun), January ice extent (54-55°N) which was also highly correlated with iceberg numbers, and January ice extent south of 55°N.

Table 5.1. Correlation coefficients (r) between negative air temperature, sea ice extent and icebergs (1963-1998).

	Icebergs	Sea ice 47-52°N Apr-Jun	Sea ice <55°N Apr-Jun	Sea ice 54-55°N Jan	Sea ice <55°N Jan
Icebergs		0.82	0.77	0.70	.57
Iqaluit -ve Air Temp					
Dec-Feb	0.67	0.64	0.64	0.67	0.58
Nov-May	0.61	0.64	0.69	0.71	0.65
Cartwright –ve Air Temp					
Dec-Feb	0.58	0.66	0.54	0.69	0.66
Nov-May	0.64	0.79	0.81	0.70	0.63
St. John's –ve Air Temp					
Dec-Feb	0.36	0.51	0.54	0.44	0.41
Nov-May	0.36	0.60	0.51	0.43	0.43
Sea ice extent					
54-55°N Jan	0.70	0.74			
48-52°N Feb	0.72	0.83			

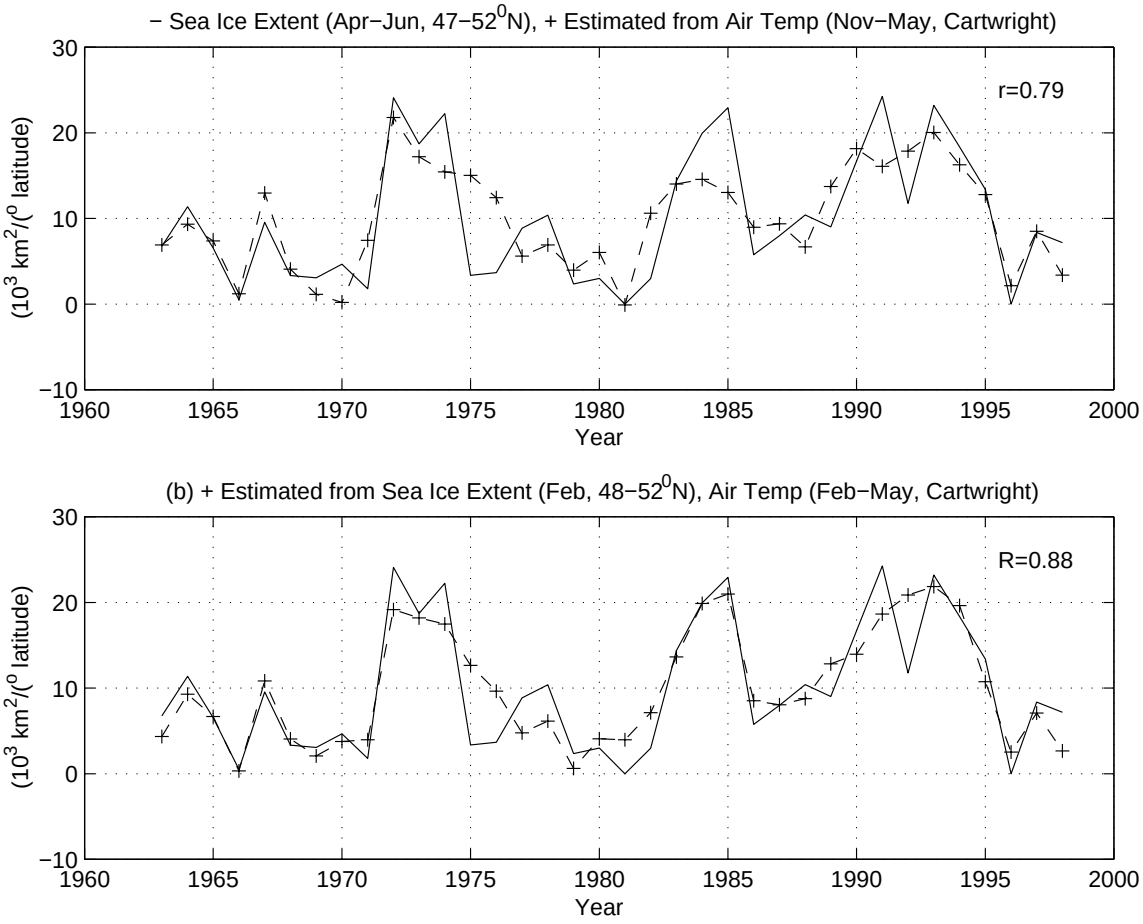

Fig. 5.1. Time series of sea ice extent (Apr-Jun, 47-52°N), and ice extent estimated from (a) Cartwright air temperature (Nov-May), and (b) sea ice extent (Feb, 48-52°N) and Cartwright air temperature (Feb-May).

Of the preceding air temperatures, Newfoundland sea ice extent from 47 to 52°N (Apr-Jun) is most highly correlated with Cartwright air temperature for the Nov-May period (r=0.79, Table 5.1). However, the correlation of sea ice extent (Apr-Jun) is even higher with February sea ice extent (r=0.83), and combined with the Feb-May Cartwright air temperature the multiple correlation coefficient (R) is 0.88. In Fig. 5.1, spring sea ice extent for 47-52°N is plotted along with the ice extent estimated from February sea ice extent and Cartwright air temperature (Feb-May) using the following regression equations:

$E_1 = -4.12 * T_1 - 18.70 \quad (r^2 = 0.63)$

$E_1 = 0.299 * E_3 - 1.405 * T_2 - 4.406 \quad (R^2 = 0.77)$

where E_1 = Sea ice extent 47-52°N (Apr-Jun)
T_1 = Air temperature Cartwright (Nov-May)
E_3 = Sea ice extent 48-52°N (Feb)
T_2 = Air temperature Cartwright (Feb-May)

Because of autocorrelation in the time series, the correlation of spring ice extent with both February ice extent and spring air temperature is not significantly higher than with February ice extent alone.

6 Surface Wind

In this section, winter and spring surface winds are compared to air temperature, the winter NAO index and iceberg numbers. Winter mean sea level pressure maps are shown in Appendix C for reference. The surface wind (0.995 sigma level) and pressure fields were produced by the NCEP/NCAR Reanalysis project, and daily mean data were obtained for a 2.5° latitude by 2.5° longitude grid for the period 1958-1998. The data were averaged over the winter (Dec-Feb) and spring (Mar-May) seasons at each grid point. Additional fields from the NCEP dataset are presented in DeTracey and Tang (1997).

6.1 Winter

Spatial correlations between the NCEP winds, the winter NAO, and negative air temperatures at Iqaluit, Cartwright and St. John's for the winters of 1958-59 to 1996-97 are shown in Fig. 6.1.1, and are summarized in Table 6.1.1. The correlations represent the multiple correlation coefficient computed using both wind components in a multiple regression model.

As expected the maximum correlation of surface wind with the winter NAO (r=0.96) is found midway between Iceland and the Azores, the locations used to compute the winter NAO. The wind direction (251°T) is about 15 degrees to the left of the geostrophic wind component perpendicular to the line joining Iceland

and the Azores. The correlation coefficient is greater than 0.7 throughout most of the Labrador Sea, but decreases to about 0.4 at St. John's.

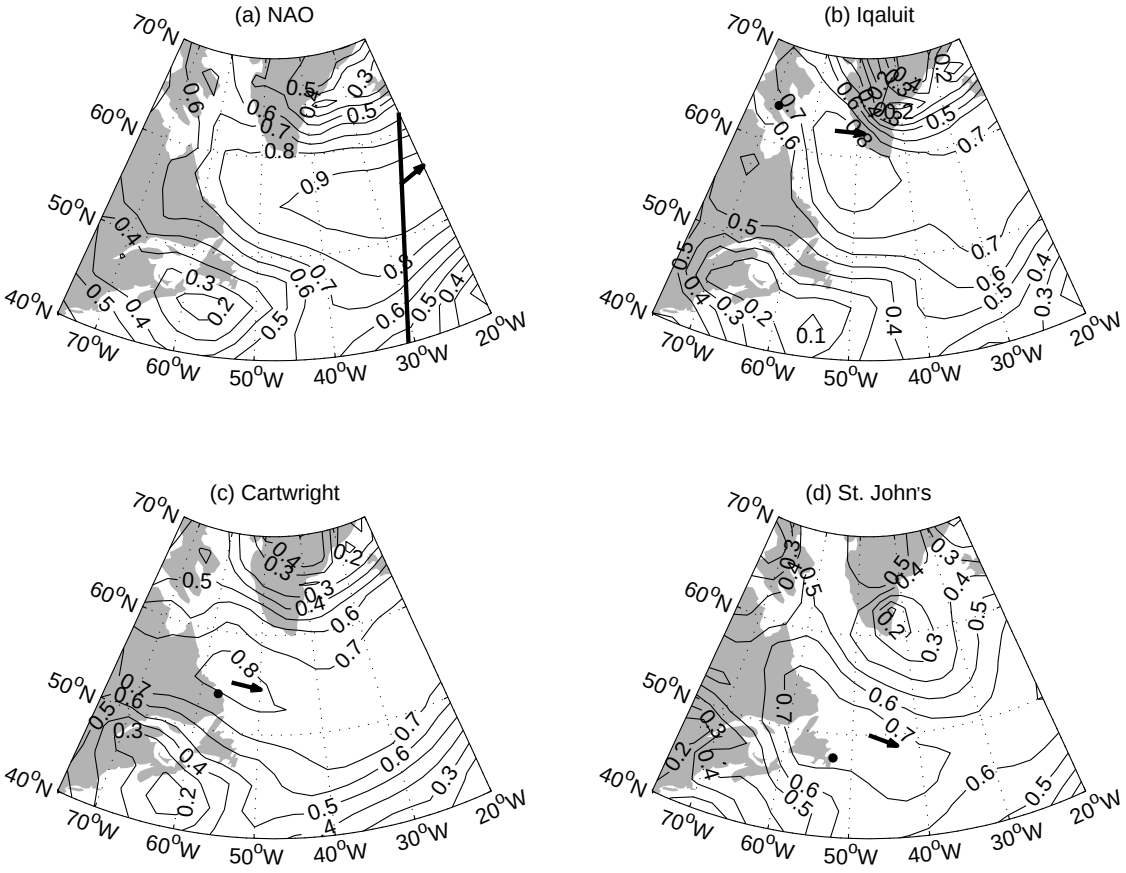

Fig. 6.1.1. Spatial correlations (r) of the winter NCEP surface winds with the winter NAO and air temperatures at Iqaluit, Cartwright and St. John's, Dec-Feb, 1959-1998. The arrows indicate the location and direction of the winds giving the maximum correlation.

Table 6.1.1. Correlation coefficients (r) between winter and spring NCEP winds, winter NAO, negative air temperature, and icebergs (1959-1998).

	Wind	Winter NAO	Icebergs
Surface Wind: Dec-Feb	1	.96	.64
NAO: Dec-Feb	.96	1	.55
Iqaluit –ve Air Temp: Dec-Feb	.87	.76	.67
Mar-May	.70		
Cartwright –ve Air Temp: Dec-Feb	.85	.71	.58
Mar-May	.57		
St. John's –ve Air Temp: Dec-Feb	.78	.45	.36
Mar-May	.63		

The maximum correlation with Iqaluit negative air temperature (r=0.87) is to the east of Iqaluit, with a wind direction from 269°T. For Cartwright, the maximum correlation (r=0.85) is with nearby winds northeast of Cartwright, with a

wind direction from 277°T. For St. John's, the maximum correlation (r=0.78) is with winds northeast of St. John's, with a wind direction from 291°T. Thus not surprisingly, the northerly wind component is more important for decreasing air temperature in the south than in the north.

The correlations between the NAO and negative air temperature decrease from 0.76 and 0.71 at Iqaluit and Cartwright to 0.45 at St. John's. This is consistent with the winter NAO correlations with wind, which also decrease from north to south.

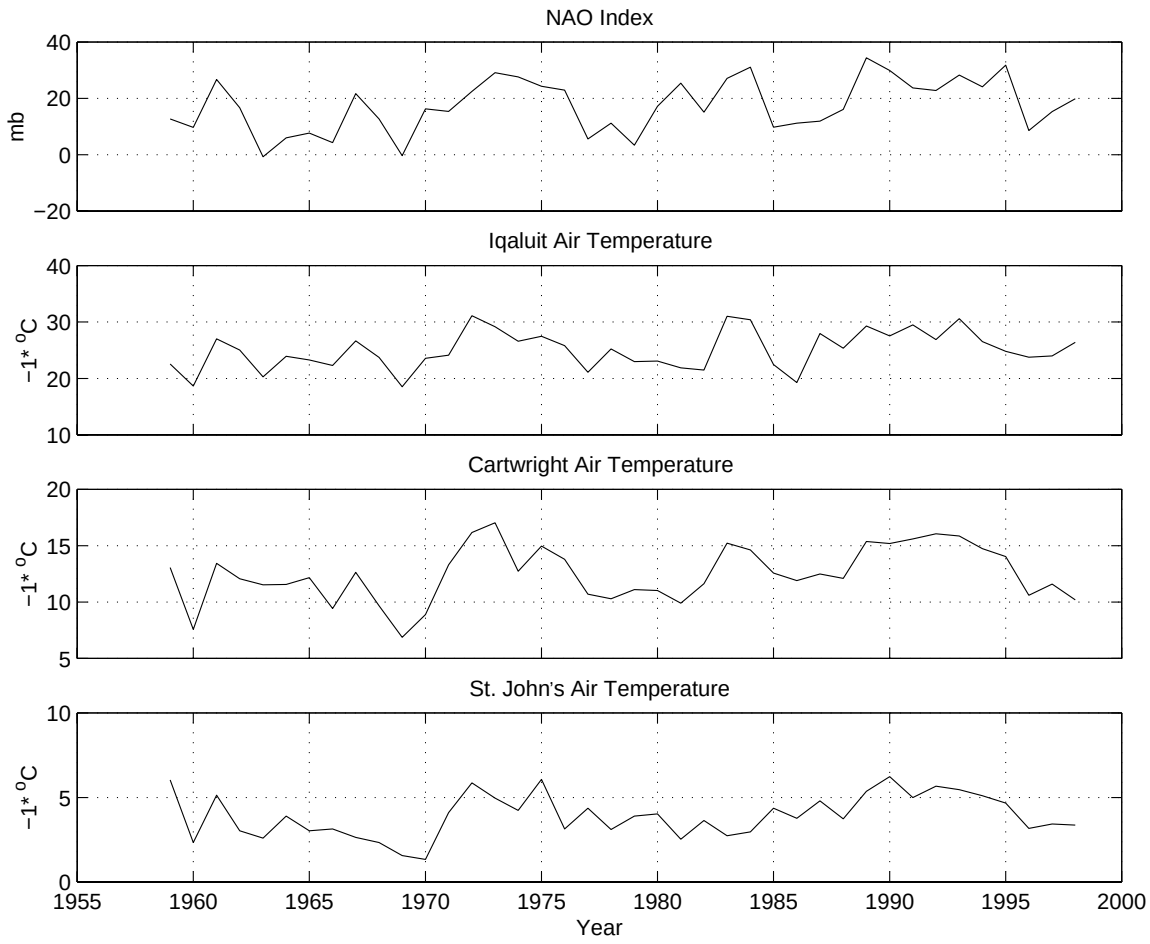

Figure 6.1.2. Time series of the winter NAO Index, and winter air temperature at Iqaluit, Cartwright and St. John's (Dec-Feb). Air temperatures have been multiplied by –1.

The time series of the winter NAO Index and air temperature at Iqaluit, Cartwright and St. John's are shown in Fig. 6.1.2, while those for the corresponding surface winds for the maximum correlation are shown in Fig. 6.1.3. Note that the air temperatures have been multiplied by –1.

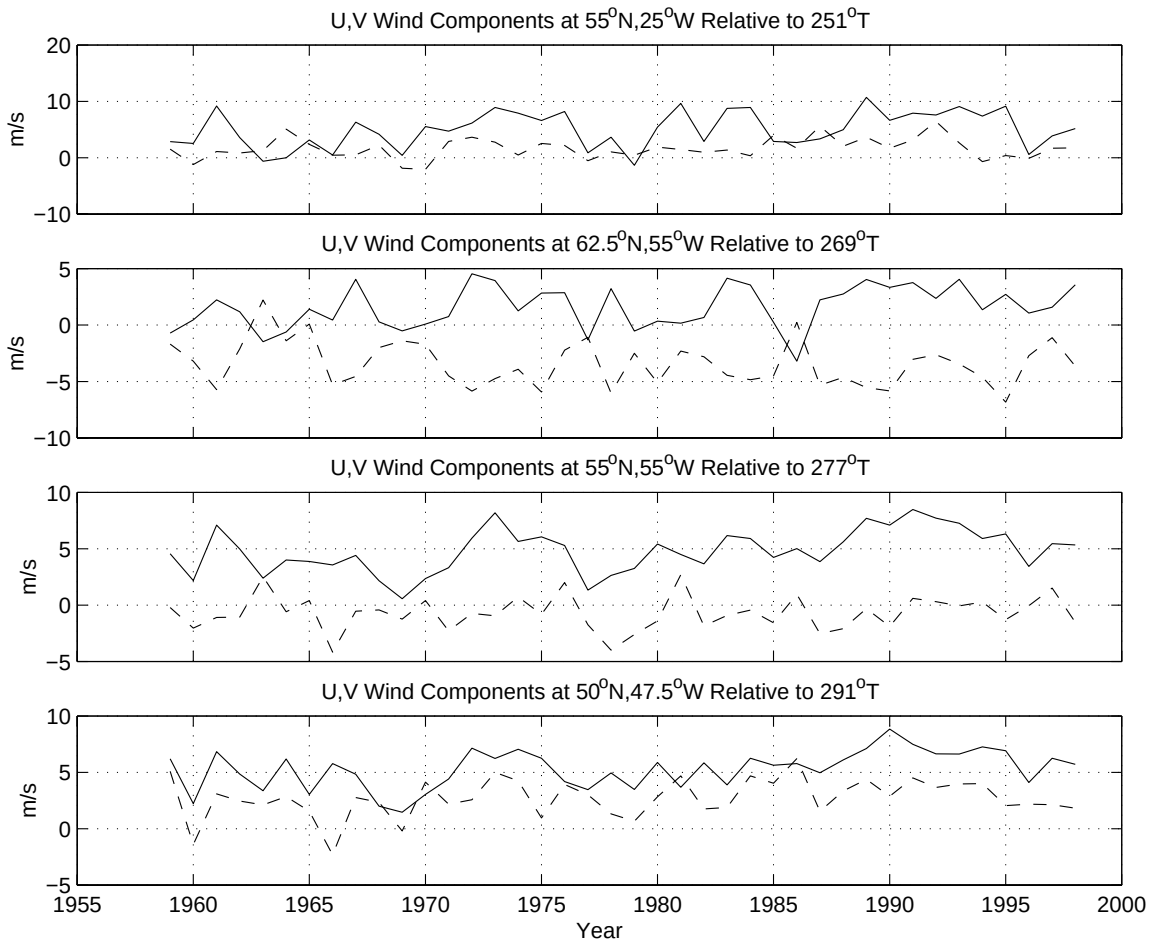

Figure 6.1.3. Time series of winter NCEP surface winds (Dec-Feb). The solid line denotes the U wind component and the dashed line denotes the V component (90° to the left of the U component). The heading of the negative U axis is printed above the plot.

Correlations between iceberg numbers and surface winds are shown in Fig. 6.1.4. The maximum correlation (0.64) is found east of the Strait of Belle Isle, with a wind direction from 278°T; the correlation between this wind component and sea ice extent (47-52°N, Apr-Jun) is also 0.64. This is in agreement with Smith (1931) who found that the barometric pressure difference giving the maximum correlation with iceberg numbers for the period 1880-1926 was between Belle Isle, Newfoundland and Ivigtut in southern Greenland from December to March (r=0.58), since it was most effective in increasing the sea ice extent. The pressure gradient between Belle Isle and Ivigtut corresponds to geostrophic winds from about 290°T, or surface winds from about 275°T.

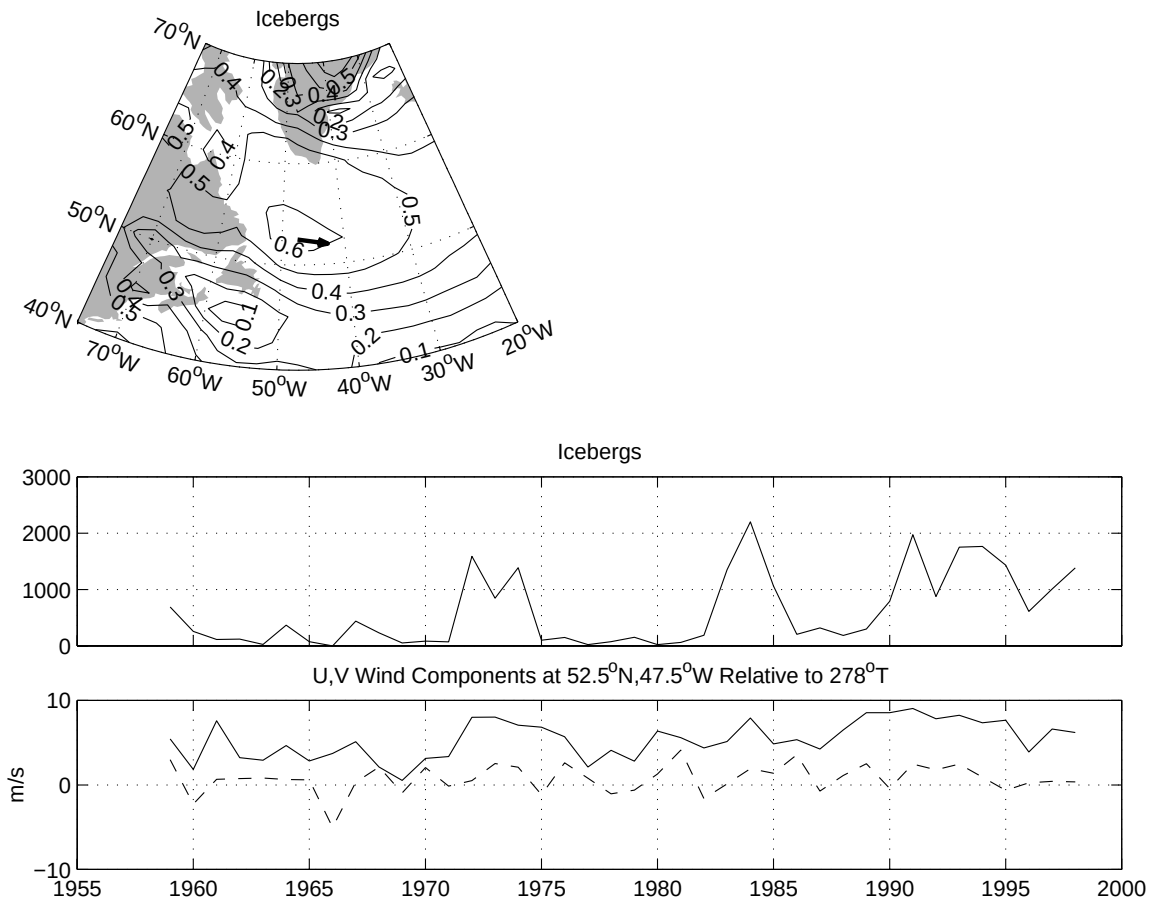

Fig. 6.1.4. Correlation coefficients (r) between winter surface wind (Dec-Feb) and iceberg numbers south of 48°N (top); time series of iceberg numbers and surface wind at 52.5°N, 47.5°W (bottom).

6.2 Spring

Spatial correlations between spring (March-May) NCEP winds and negative air temperatures at Iqaluit, Cartwright and St. John's for the winters of 1958-59 to 1996-98 are shown in Fig. 6.2.1, and are summarized in Table 6.1.1.

In general, the correlations for spring are lower than for winter, and the northerly wind component is more important in producing cold air temperatures. The maximum correlation with Iqaluit negative air temperature (r=0.70) is to the southeast of Iqaluit, with a wind direction from 311°T. For Cartwright, the maximum correlation (r=0.57) is with nearby winds northeast of Cartwright, with a wind direction from 307°T. For St. John's, the maximum correlation (r=0.63) is with local winds with a wind direction from 306°T.

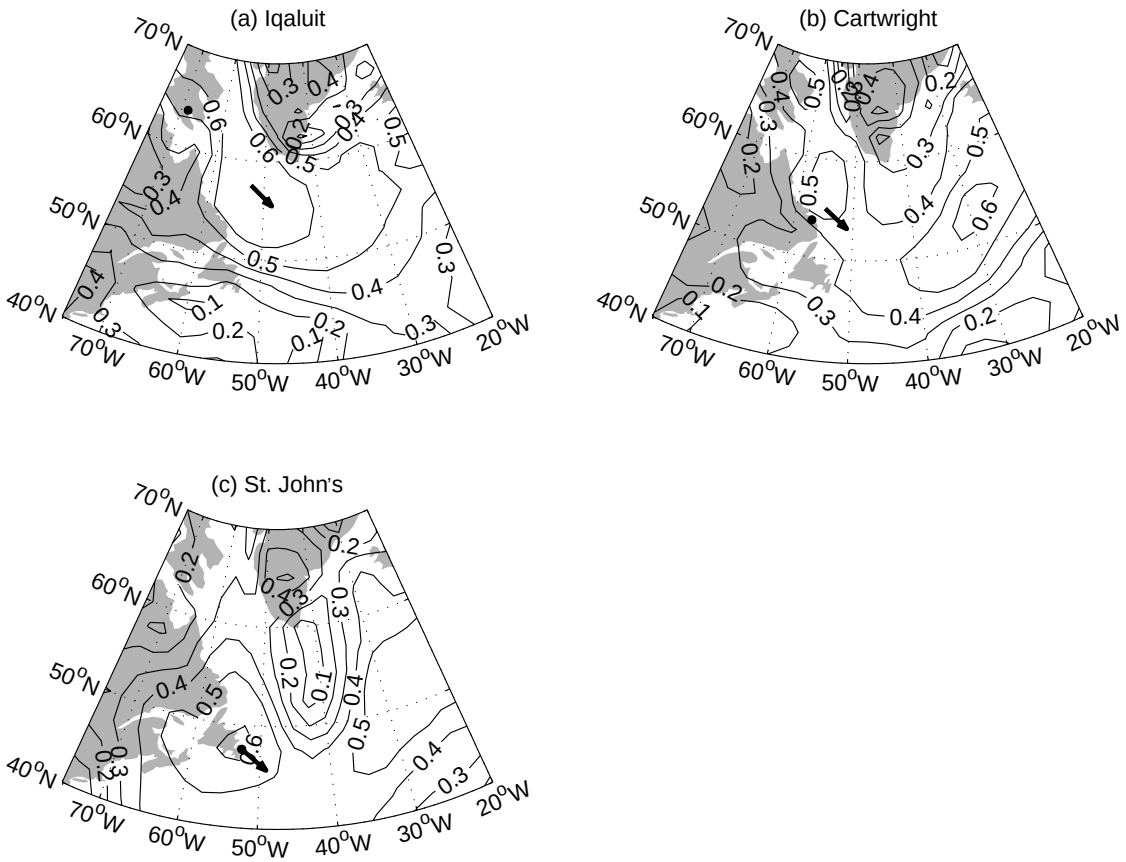

Fig. 6.2.1. Spatial correlations (r) of the spring NCEP surface winds with the negative air temperatures at Iqaluit, Cartwright and St. John's, Mar-May, 1959-1998. The arrows indicate the location and direction (to) of the winds giving the maximum correlation.

The time series for the air temperature at Iqaluit, Cartwright and St. John's are shown in Fig. 6.2.2, while those for the corresponding surface winds for the maximum correlation are shown in Fig. 6.2.3.

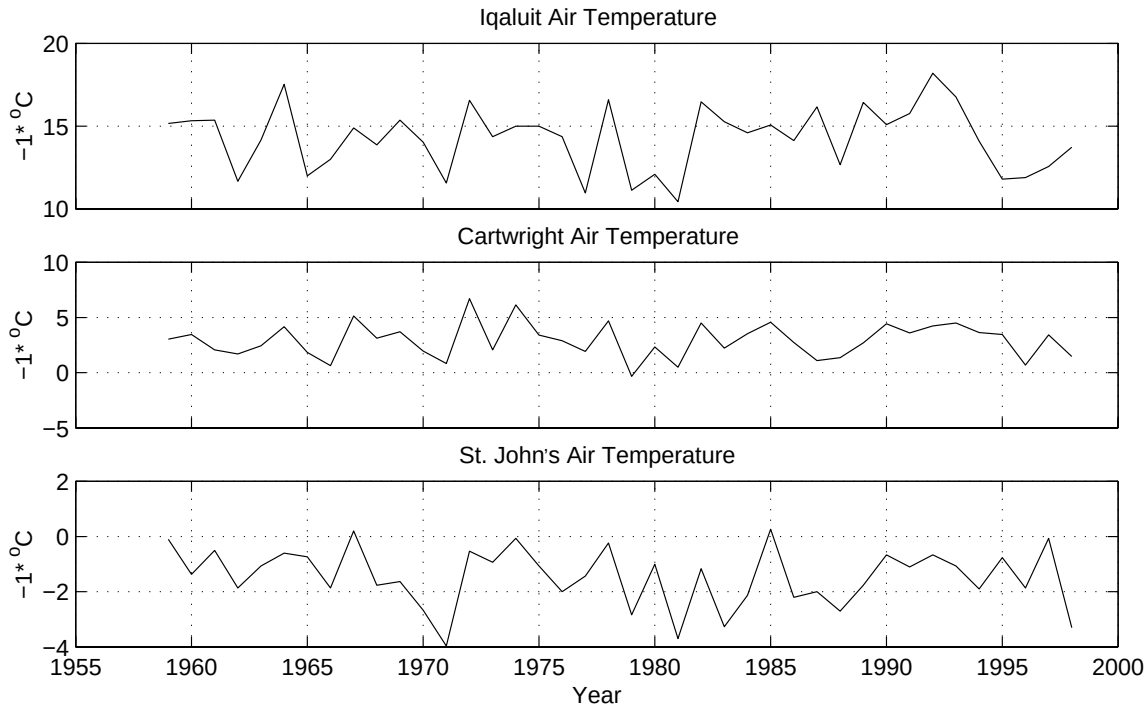

Figure 6.2.2. Time series of spring air temperature (multiplied by –1) at Iqaluit, Cartwright and St. John's (Mar-May).

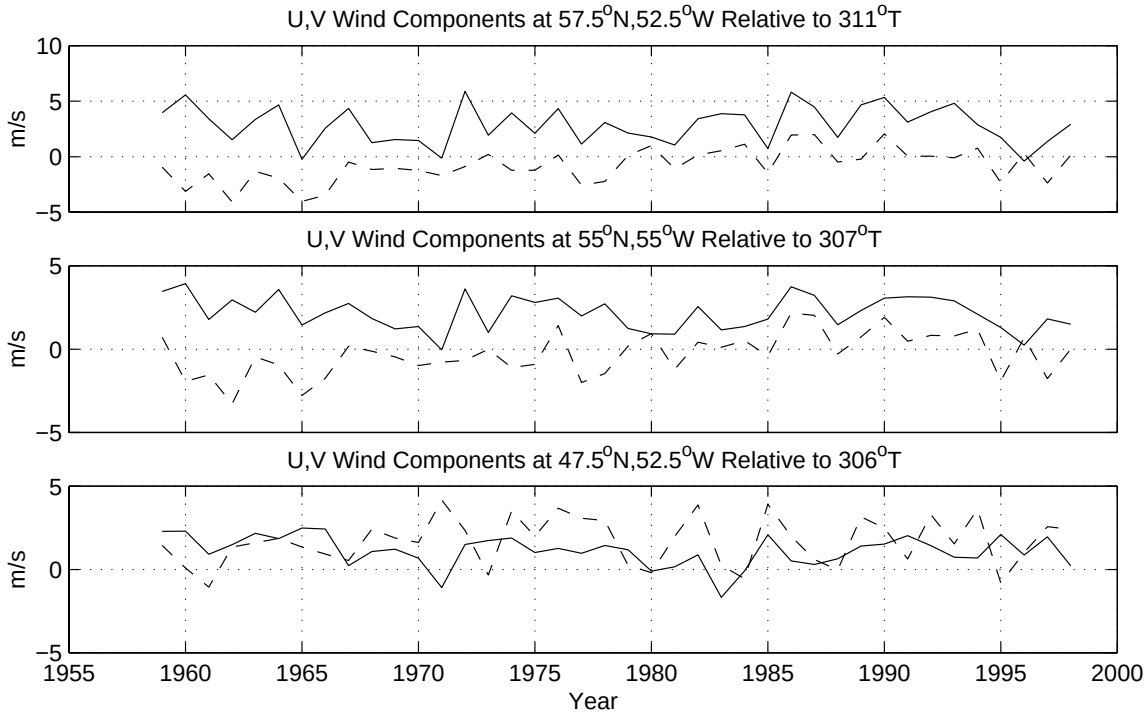

Figure 6.2.3. Time series of NCEP surface winds (Mar-May). The solid line denotes the U wind component and the dashed line denotes the V component (90° to the left of the U component). The heading of the negative U axis is printed above the plot.

7 Conclusions

1) Sea ice extent anomalies in the western Labrador Sea are presented for the period, 1963-1998. Since 1988, ice extent was highest in 1990 and 1993 north of 58°N, while south of 55°N, ice extent was high throughout 1990 to 1994.

2) The annual number of icebergs drifting south of 48°N is most strongly correlated with sea ice extent off Newfoundland between 47 and 52°N from Apr 1 – June 1 (r=0.82). This can easily be explained since most icebergs drift south of 48°N from April to June, and are most likely to be present over the portion of the shelf at 48°N covered by sea ice, where they are in colder water and are protected from wave erosion. For January sea ice, correlations with annual iceberg numbers are high both off Hudson Strait and off Cartwright (r=0.70). These results corroborate findings by Smith (1931) and Marko et al (1986,1994) in greater spatial and temporal detail.

3) Iqaluit negative air temperatures from December to February are highly correlated with sea ice extent north of 58°N 0-4 months later. Similarly, Cartwright negative winter air temperatures are highly correlated with sea ice extent over the Northeast Newfoundland Shelf. Negative air temperatures in both regions from March to May are correlated to a lesser degree with sea ice extent 0-2 months later. Newfoundland sea ice extent from 47 to 52°N (Apr-Jun) is most highly correlated with a combination of sea ice extent from 48 to 52°N (Feb) and Cartwright Feb-May negative air temperature (r=0.88), while the correlation with negative air temperature alone (Nov-May) is 0.79.

4) Because of the high persistence of sea ice, the best predictor of both spring sea ice extent (Apr-Jun) and iceberg numbers south of 48°N is sea ice extent several months earlier. January sea ice extent accounts for 55% and 49% of the variance of spring ice extent and iceberg numbers respectively, while February sea ice extent accounts for 69% and 53%.

5) Local surface winds account for 76%, 72% and 61% of the variance of winter air temperature at Iqaluit, Cartwright and St. John's respectively, compared to the winter North Atlantic Oscillation index which accounts for 58%, 50% and 20%. Cold temperatures are associated with westerly or west-northwesterly winds in winter and northwesterly winds in spring.

8 Acknowledgements

We wish to thank the Canadian Ice Service for providing ice charts, Ken Drinkwater and Roger Pettipas for air temperature and NAO data, and Tom Yao and Ken Drinkwater for reviewing the manuscript.

9 References

Anderson, I. 1993, "International Ice Patrol Iceberg Sighting Data Base 1960-1991", Appendix D in Report of the International Ice Patrol in the North Atlantic, Bulletin No. 79, 1993 Season, CG-188-48, Washington, DC.

Atmospheric Environment Service, 1992. MANIS Manual of Ice Services. Environment Canada, 64 pp.

Cote, P.W. 1989. Ice limits Eastern Canadian Seaboard. Atmospheric Environment Service, 39 pp.

DeTracey, B.M. and C.L. Tang. 1997. Monthly climatological atlas of surface atmospheric conditions of the Northwest Atlantic. Can. Data Rep. Hydrogr. Ocean Sci. 152:iv+63 pp.

Drinkwater, K.F. 1995. Overview of environmental conditions in the Northwest Atlantic in 1993. NAFO Sci. Coun. Studies 23:9-42.

Manak, D.K. and L.A. Mysak. 1987. Climatic atlas of Arctic sea ice extent and anomalies, 1953-1984. Climate Res. Group Report 87-8, Dept. of Meteorology, McGill University, Montreal, Que., 214 pp.

Markham, W.E. 1980. Ice atlas Eastern Canadian Seaboard. Atmospheric Environment Service, 96 pp.

Markham, W.E. 1988. Ice atlas Hudson Bay and approaches. Atmospheric Environment Service, 123 pp.

Marko, J.R., D.B. Fissel,and J.R.Birch. 1986. Physical approaches to iceberg severity prediction. ESRF Report No. 038, 104 pp.

Marko, J.R.,D.B. Fissel, P. Wadhams, P.M. Kelly, and R.D. Brown. 1994. Iceberg severity off Eastern North America: Its relationship to sea ice variability and climate change. J. Climate 7: 1335-1351.

Peterson, I.K. and S. J. Prinsenberg. 1990. Sea ice fluctuations in the western Labrador Sea (1963-1988). Can. Tech. Rep. Hydrogr. Ocean Sci. No. 123:iv + 130 pp.

Prinsenberg, S.J., I.K. Peterson, S. Narayanan, S. and J.U.Umoh. 1997. Interaction between Atmosphere, Ice Cover and Ocean off Labrador and Newfoundland from 1962 to 1992. Can. J. Fish. Aquat. Sci. 54(Suppl. 1):30-39.

Robe, R.Q. 1980. Iceberg drift and deterioration, In: Colbeck, S.C. (ed.) Dynamics of Snow and Ice Masses. New York, Academic Press, pp. 211-259.

Smith, E.H. 1931. The Marion Expedition to Davis Strait and Baffin Bay, 1928. U.S. Coast Guard Bull. No. 19, Part 3, 221 p.

Sowden, W.J. and F.E. Geddes. 1980. Weekly median and extreme ice edges for the Canadian seaboard and Hudson Bay. Atmospheric Environment Service.

Walsh, J.E. and C.M. Johnson. 1979. Interannual atmospheric variability and associated fluctuations in Arctic sea ice extent. J. Geophys. Res. 84: 6915-6928.

APPENDIX A

Monthly median ice concentrations, fraction of first year ice, minimum and maximum ice concentrations, 1963-1998

Median ice concentrations at the start of each month for each grid cell, 1963-1998 (upper left). Only grid cells for which the coverage is greater than 50% are included. The 300, 1000, and 3000 m bottom contours are also shown.

Median fraction of first-year ice at the start of each month for each grid cell (upper right). First year ice is >30 cm. The median is computed over all years in which the coverage is greater than 50% in the given month and grid cell.

Minimum ice concentration at the start of each month for each grid cell (lower left).

Maximum concentration at the start of each month for each grid cell (lower right).

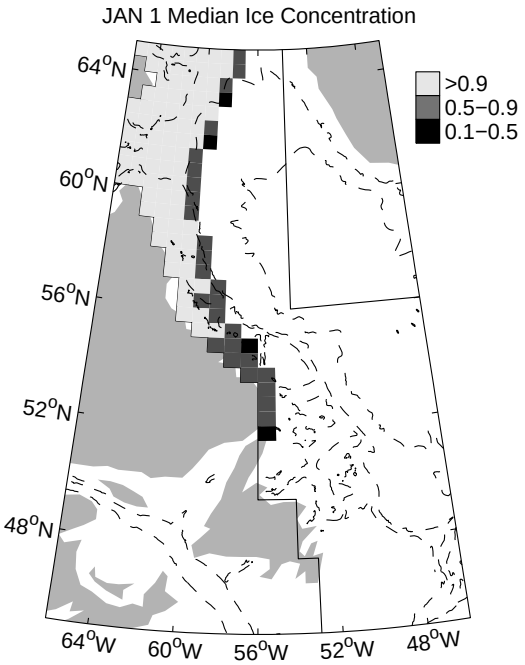
JAN 1 Median Ice Concentration
>0.9
0.5−0.9
0.1−0.5
64°N
60°N
56°N
52°N
48°N
64°W
60°W
56°W
52°W
48°W

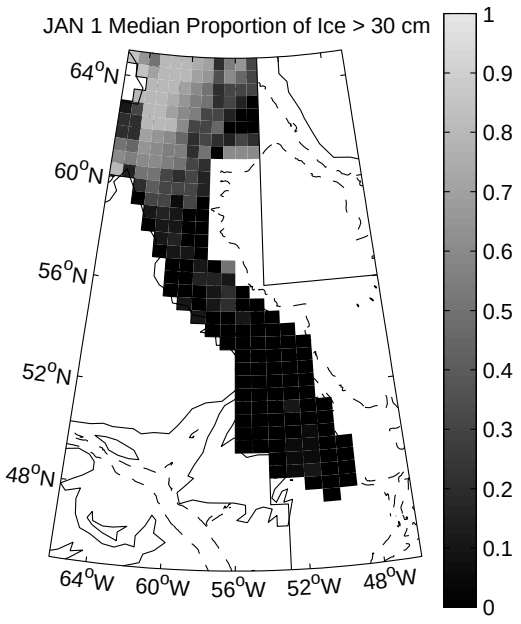
JAN 1 Median Proportion of Ice > 30 cm
1
0.9
0.8
0.7
0.6
0.5
0.4
0.3
0.2
0.1
0
64°N
60°N
56°N
52°N
48°N
64°W
60°W
56°W
52°W
48°W

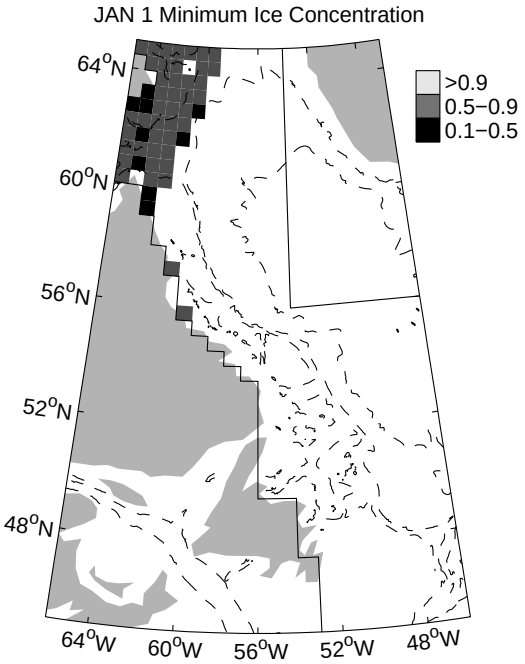
JAN 1 Minimum Ice Concentration
>0.9
0.5−0.9
0.1−0.5
64°N
60°N
56°N
52°N
48°N
64°W
60°W
56°W
52°W
48°W

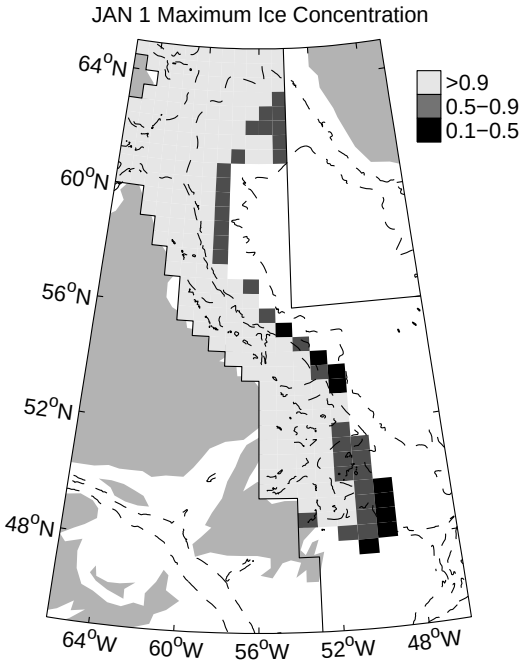
JAN 1 Maximum Ice Concentration
>0.9
0.5−0.9
0.1−0.5
64°N
60°N
56°N
52°N
48°N
64°W
60°W
56°W
52°W
48°W

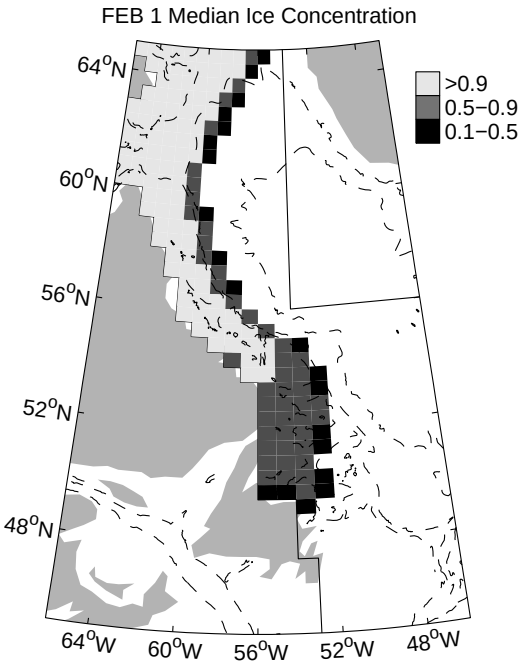
FEB 1 Median Ice Concentration
>0.9
0.5−0.9
0.1−0.5
64°N
60°N
56°N
52°N
48°N
64°W
60°W
56°W
52°W
48°W

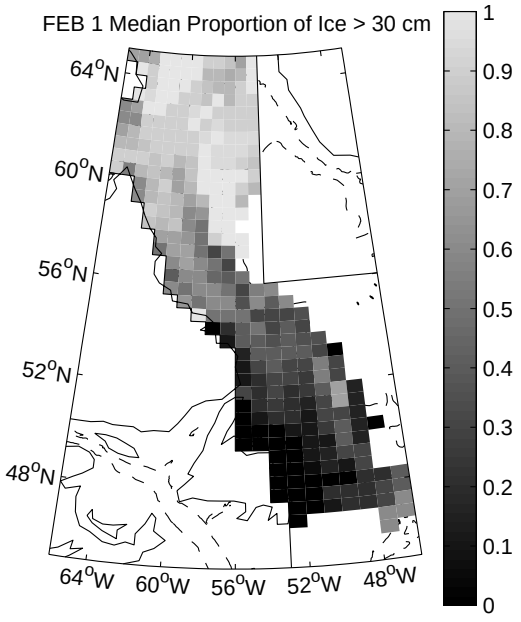
FEB 1 Median Proportion of Ice > 30 cm
1
0.9
0.8
0.7
0.6
0.5
0.4
0.3
0.2
0.1
0
64°N
60°N
56°N
52°N
48°N
64°W
60°W
56°W
52°W
48°W

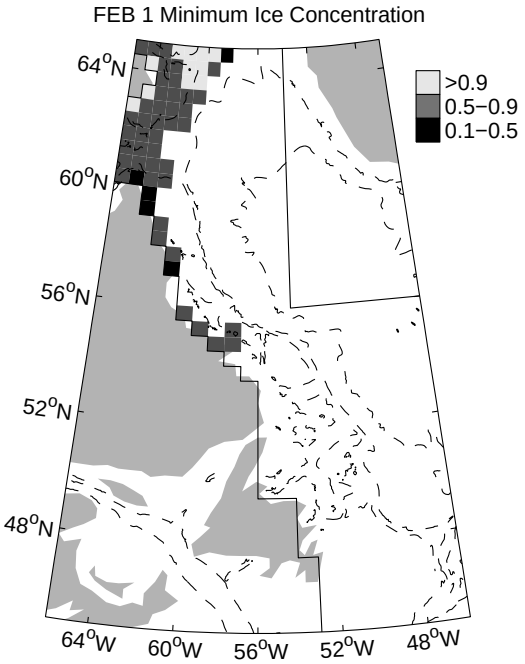
FEB 1 Minimum Ice Concentration
>0.9
0.5−0.9
0.1−0.5
64°N
60°N
56°N
52°N
48°N
64°W
60°W
56°W
52°W
48°W

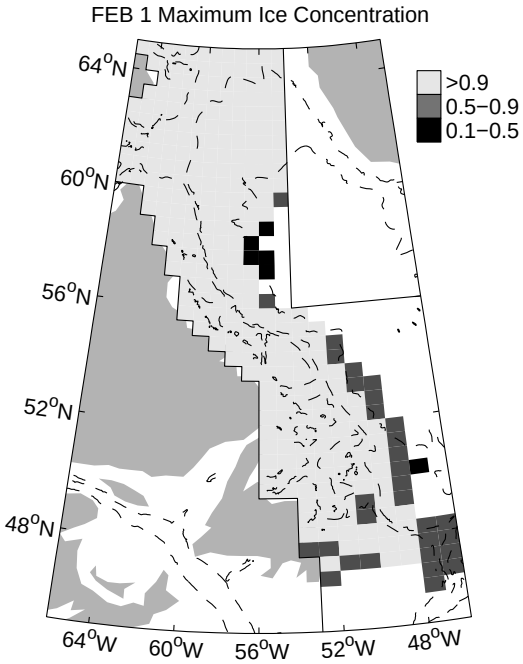
FEB 1 Maximum Ice Concentration
>0.9
0.5−0.9
0.1−0.5
64°N
60°N
56°N
52°N
48°N
64°W
60°W
56°W
52°W
48°W

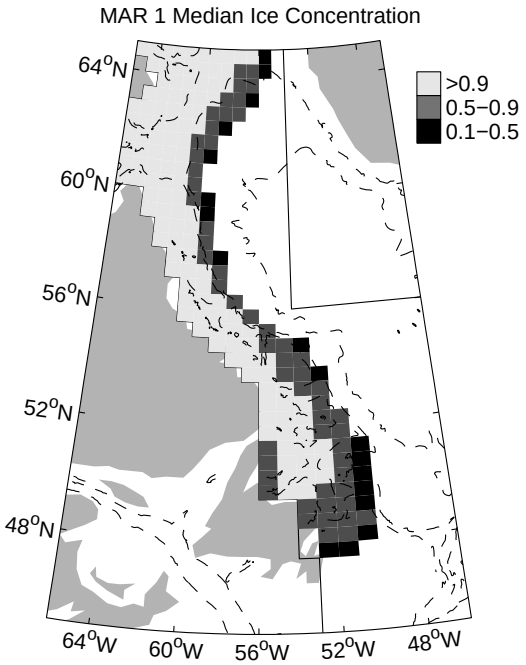
MAR 1 Median Ice Concentration
>0.9
0.5−0.9
0.1−0.5
64°N
60°N
56°N
52°N
48°N
64°W
60°W
56°W
52°W
48°W

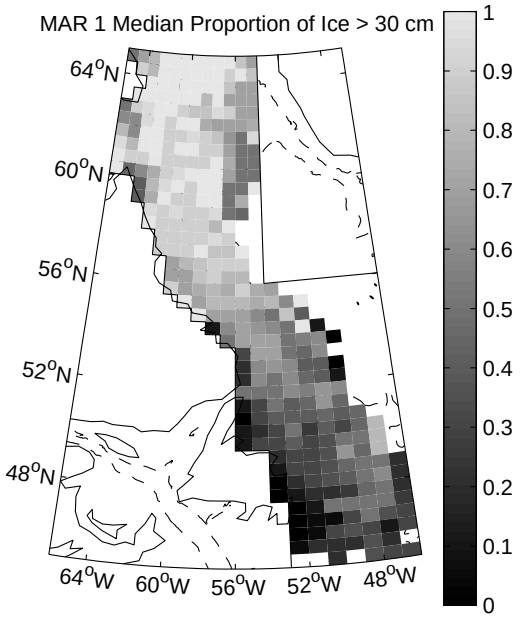
MAR 1 Median Proportion of Ice > 30 cm
1
0.9
0.8
0.7
0.6
0.5
0.4
0.3
0.2
0.1
0
64°N
60°N
56°N
52°N
48°N
64°W
60°W
56°W
52°W
48°W

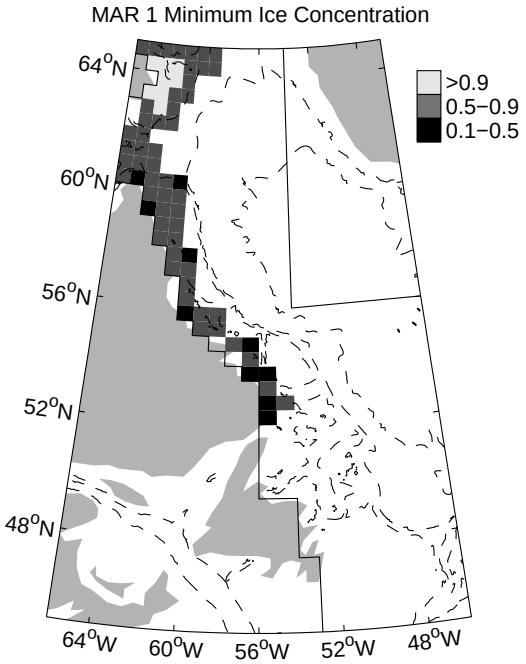
MAR 1 Minimum Ice Concentration
>0.9
0.5−0.9
0.1−0.5
64°N
60°N
56°N
52°N
48°N
64°W
60°W
56°W
52°W
48°W

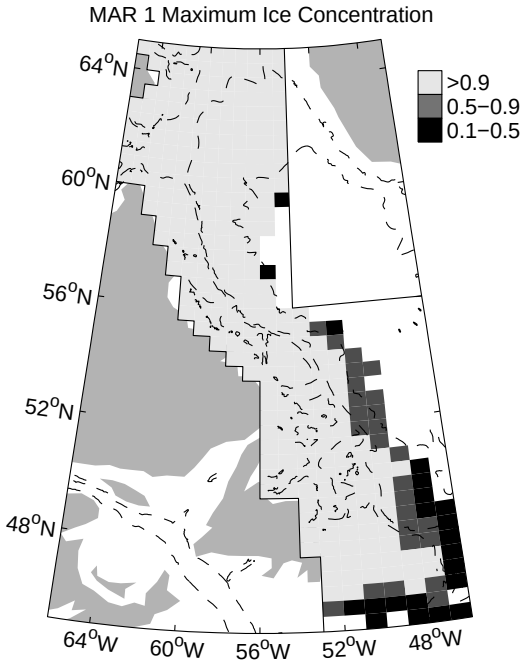
MAR 1 Maximum Ice Concentration
>0.9
0.5−0.9
0.1−0.5
64°N
60°N
56°N
52°N
48°N
64°W
60°W
56°W
52°W
48°W

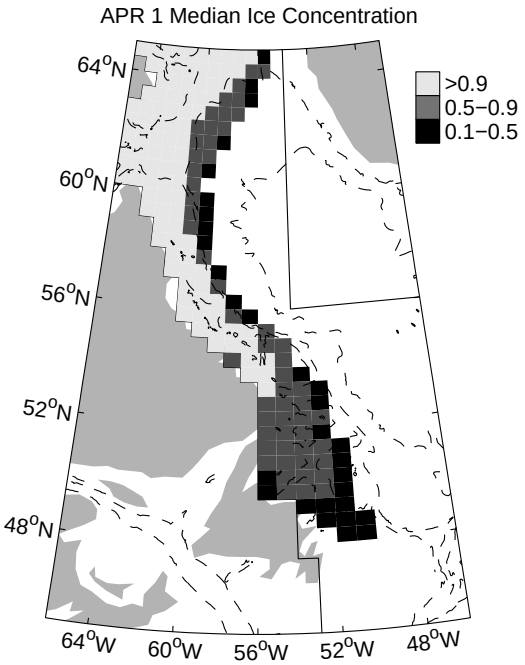
APR 1 Median Ice Concentration
64°N
60°N
56°N
52°N
48°N
64°W
60°W
56°W
52°W
48°W
>0.9
0.5−0.9
0.1−0.5

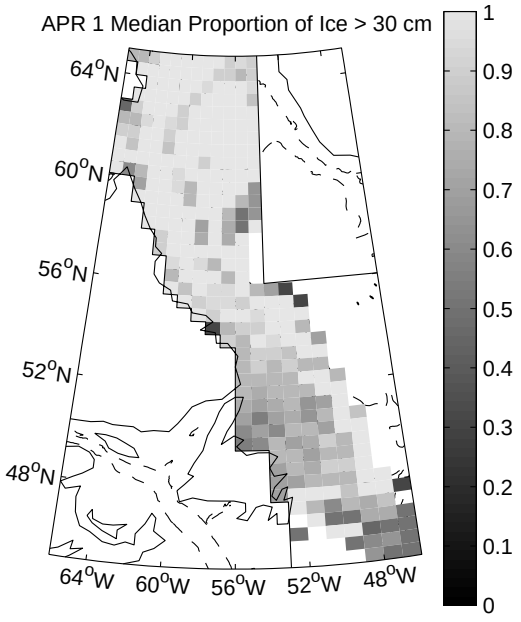
APR 1 Median Proportion of Ice > 30 cm
64°N
60°N
56°N
52°N
48°N
64°W
60°W
56°W
52°W
48°W
1
0.9
0.8
0.7
0.6
0.5
0.4
0.3
0.2
0.1
0

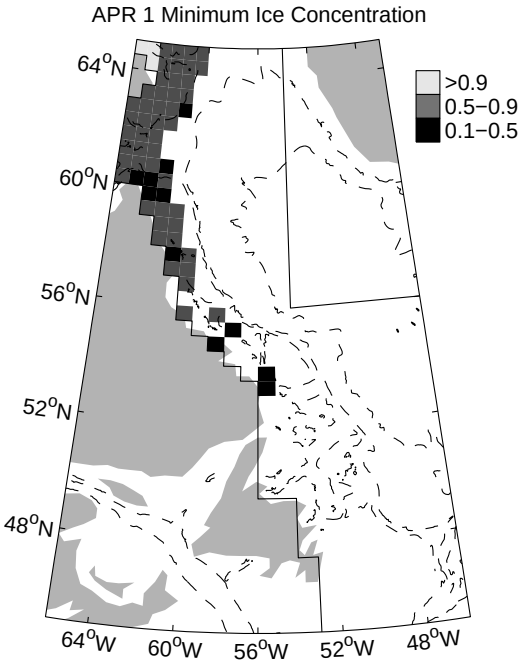
APR 1 Minimum Ice Concentration
64°N
60°N
56°N
52°N
48°N
64°W
60°W
56°W
52°W
48°W
>0.9
0.5−0.9
0.1−0.5

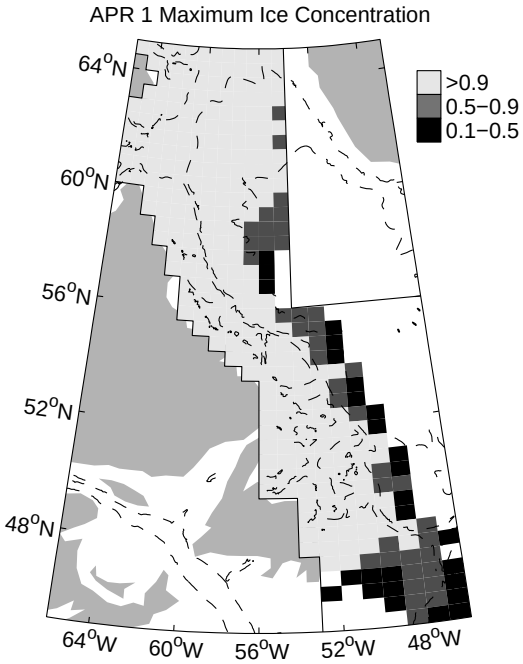
APR 1 Maximum Ice Concentration
64°N
60°N
56°N
52°N
48°N
64°W
60°W
56°W
52°W
48°W
>0.9
0.5−0.9
0.1−0.5

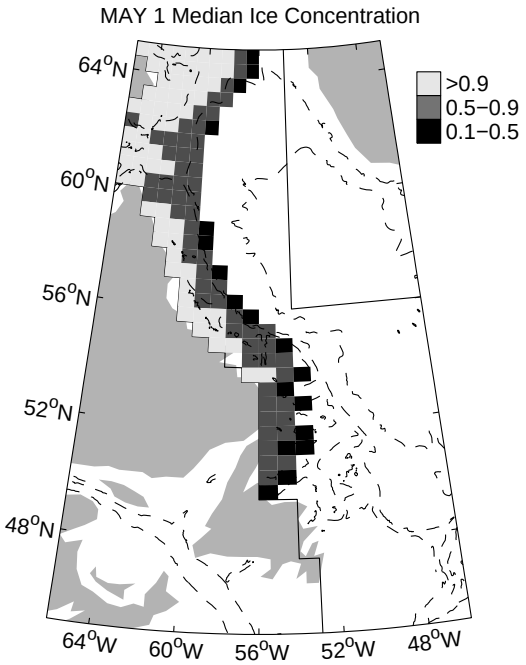
MAY 1 Median Ice Concentration
64°N
60°N
56°N
52°N
48°N
64°W
60°W
56°W
52°W
48°W
>0.9
0.5−0.9
0.1−0.5

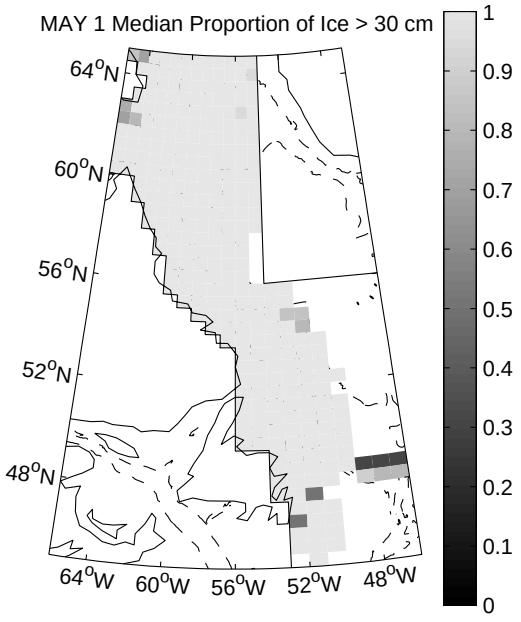
MAY 1 Median Proportion of Ice > 30 cm
64°N
60°N
56°N
52°N
48°N
64°W
60°W
56°W
52°W
48°W
1
0.9
0.8
0.7
0.6
0.5
0.4
0.3
0.2
0.1
0

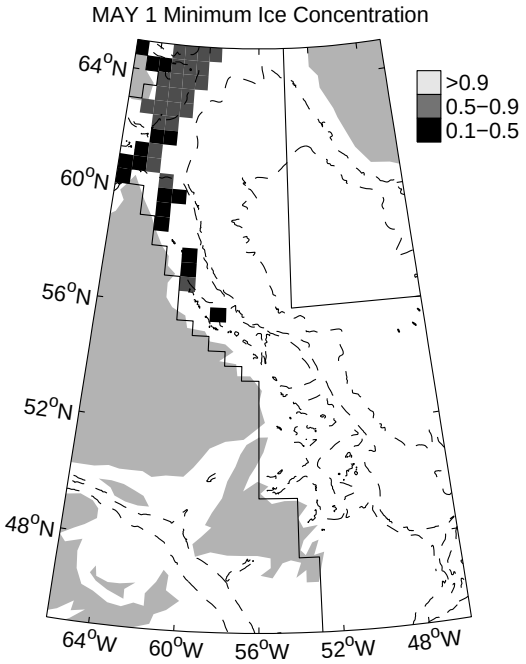
MAY 1 Minimum Ice Concentration
64°N
60°N
56°N
52°N
48°N
64°W
60°W
56°W
52°W
48°W
>0.9
0.5−0.9
0.1−0.5

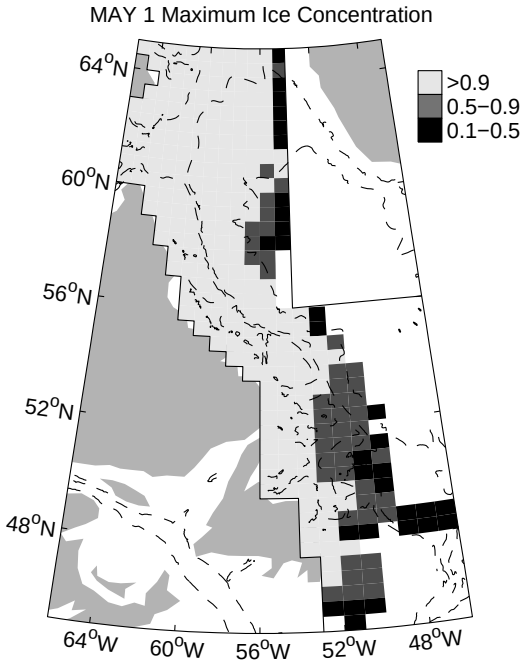
MAY 1 Maximum Ice Concentration
64°N
60°N
56°N
52°N
48°N
64°W
60°W
56°W
52°W
48°W
>0.9
0.5−0.9
0.1−0.5

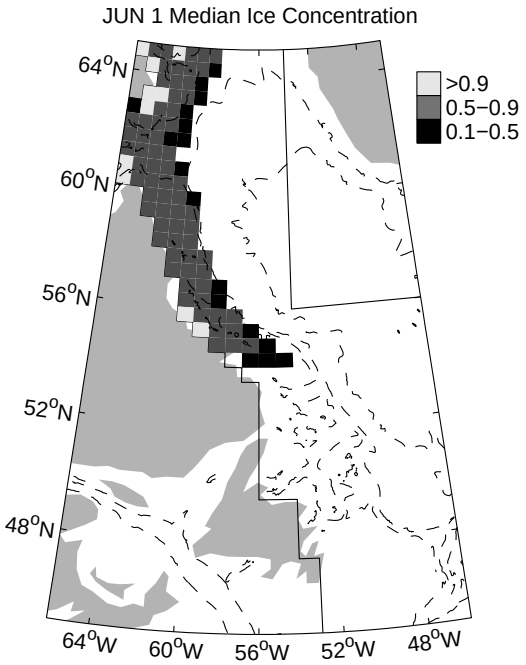
JUN 1 Median Ice Concentration
>0.9
0.5−0.9
0.1−0.5
64°N
60°N
56°N
52°N
48°N
64°W
60°W
56°W
52°W
48°W

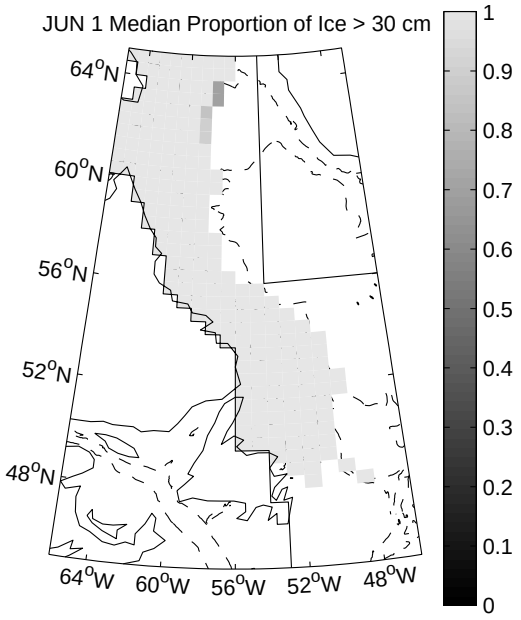
JUN 1 Median Proportion of Ice > 30 cm
1
0.9
0.8
0.7
0.6
0.5
0.4
0.3
0.2
0.1
0
64°N
60°N
56°N
52°N
48°N
64°W
60°W
56°W
52°W
48°W

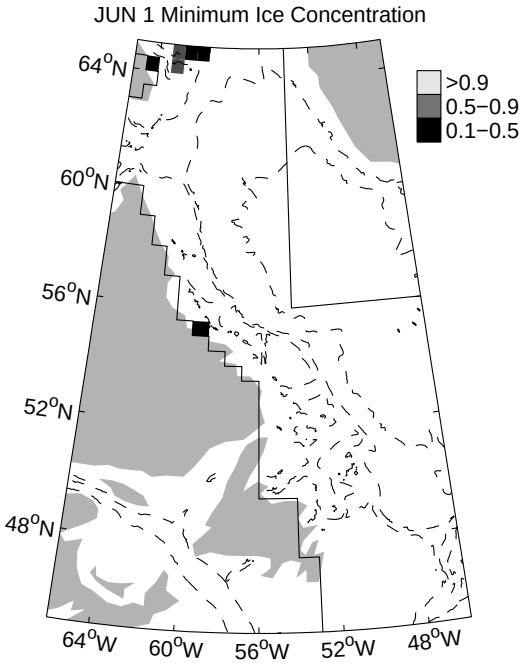
JUN 1 Minimum Ice Concentration
>0.9
0.5−0.9
0.1−0.5
64°N
60°N
56°N
52°N
48°N
64°W
60°W
56°W
52°W
48°W

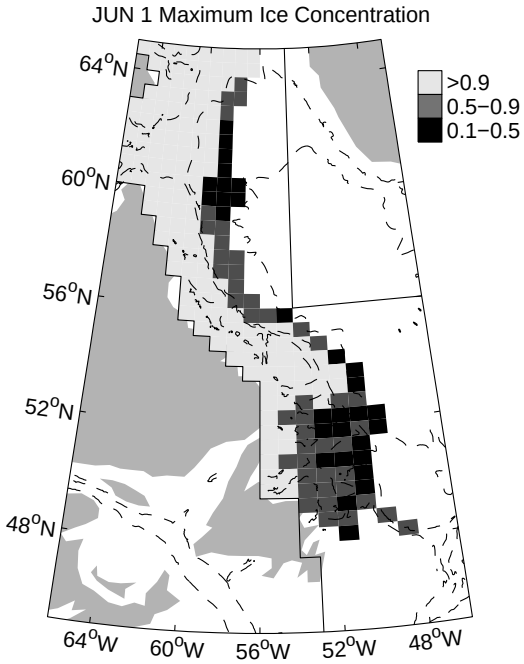
JUN 1 Maximum Ice Concentration
>0.9
0.5−0.9
0.1−0.5
64°N
60°N
56°N
52°N
48°N
64°W
60°W
56°W
52°W
48°W

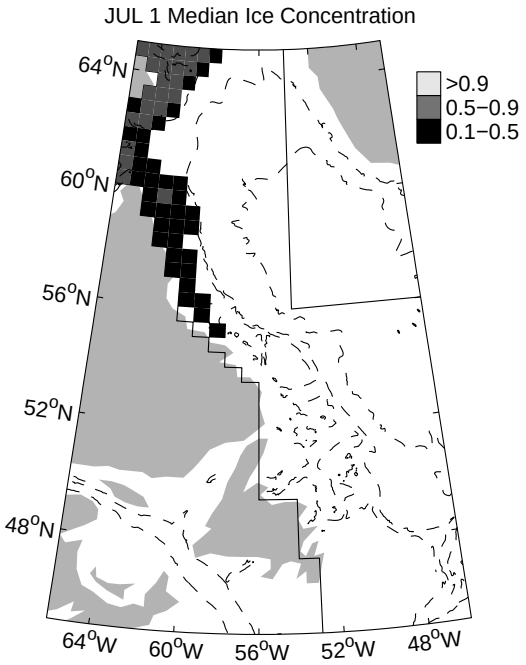
JUL 1 Median Ice Concentration
>0.9
0.5−0.9
0.1−0.5
64°N
60°N
56°N
52°N
48°N
64°W
60°W
56°W
52°W
48°W

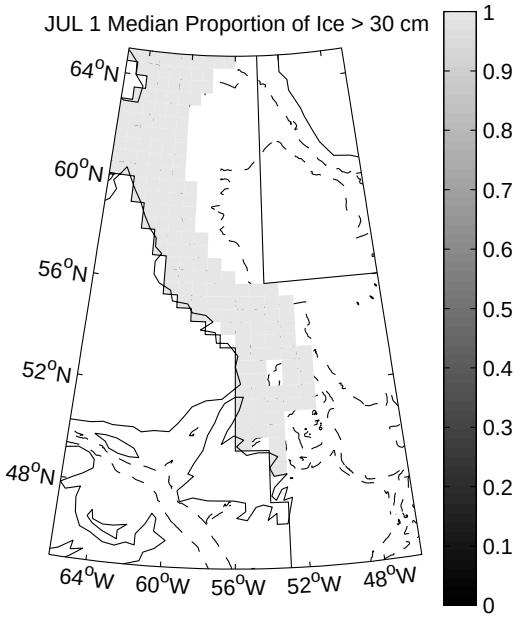
JUL 1 Median Proportion of Ice > 30 cm
1
0.9
0.8
0.7
0.6
0.5
0.4
0.3
0.2
0.1
0
64°N
60°N
56°N
52°N
48°N
64°W
60°W
56°W
52°W
48°W

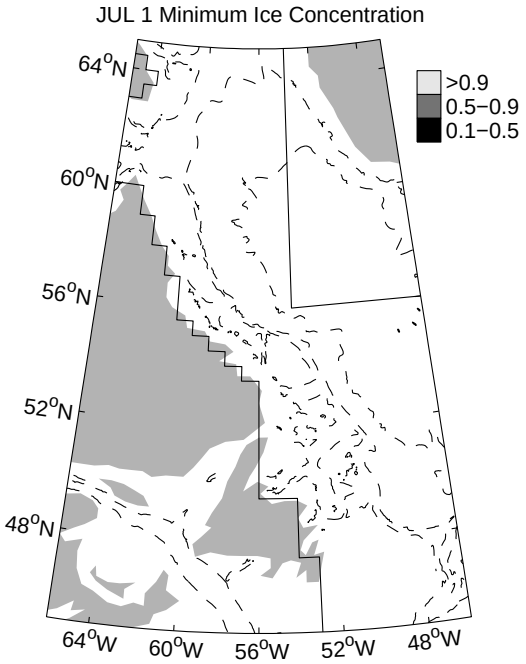
JUL 1 Minimum Ice Concentration
>0.9
0.5−0.9
0.1−0.5
64°N
60°N
56°N
52°N
48°N
64°W
60°W
56°W
52°W
48°W

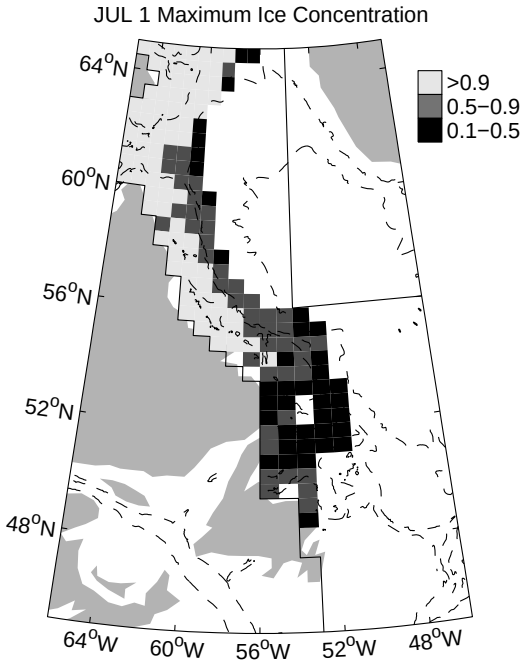
JUL 1 Maximum Ice Concentration
>0.9
0.5−0.9
0.1−0.5
64°N
60°N
56°N
52°N
48°N
64°W
60°W
56°W
52°W
48°W

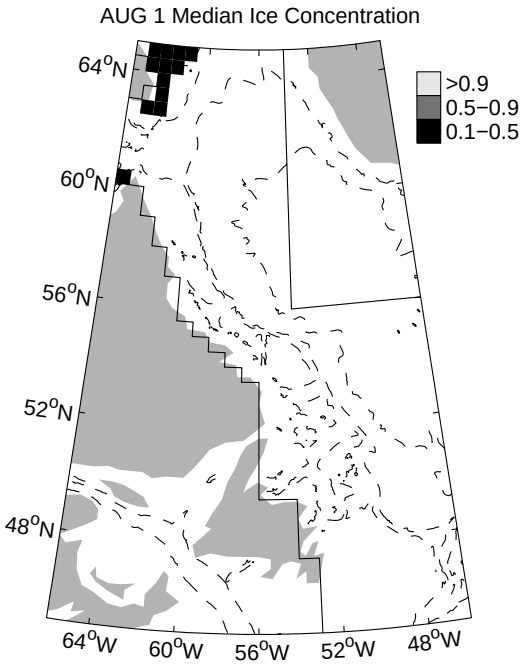
AUG 1 Median Ice Concentration
>0.9
0.5−0.9
0.1−0.5
64°N
60°N
56°N
52°N
48°N
64°W
60°W
56°W
52°W
48°W

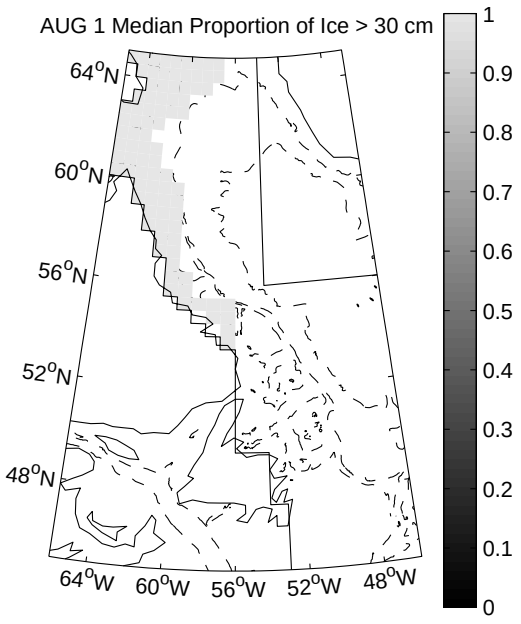
AUG 1 Median Proportion of Ice > 30 cm
1
0.9
0.8
0.7
0.6
0.5
0.4
0.3
0.2
0.1
0
64°N
60°N
56°N
52°N
48°N
64°W
60°W
56°W
52°W
48°W

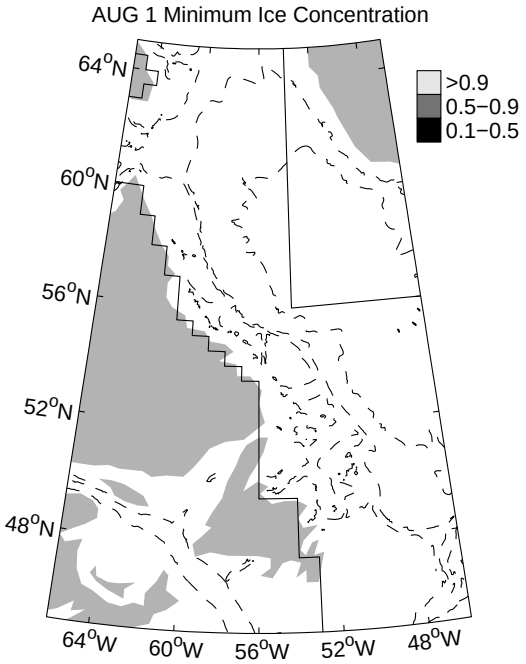
AUG 1 Minimum Ice Concentration
>0.9
0.5−0.9
0.1−0.5
64°N
60°N
56°N
52°N
48°N
64°W
60°W
56°W
52°W
48°W

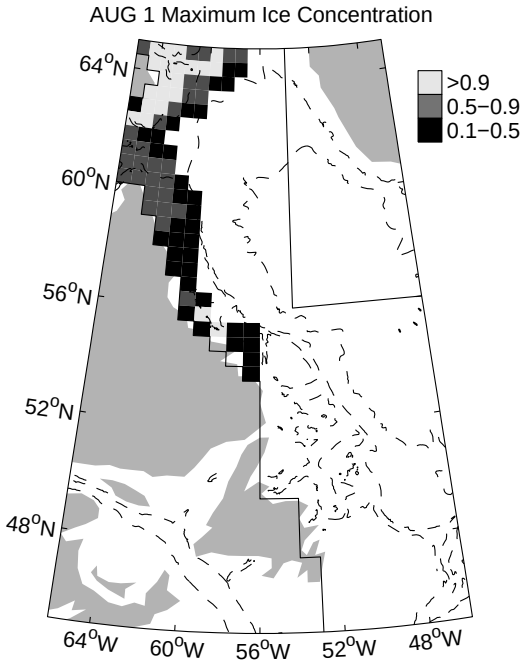
AUG 1 Maximum Ice Concentration
>0.9
0.5−0.9
0.1−0.5
64°N
60°N
56°N
52°N
48°N
64°W
60°W
56°W
52°W
48°W

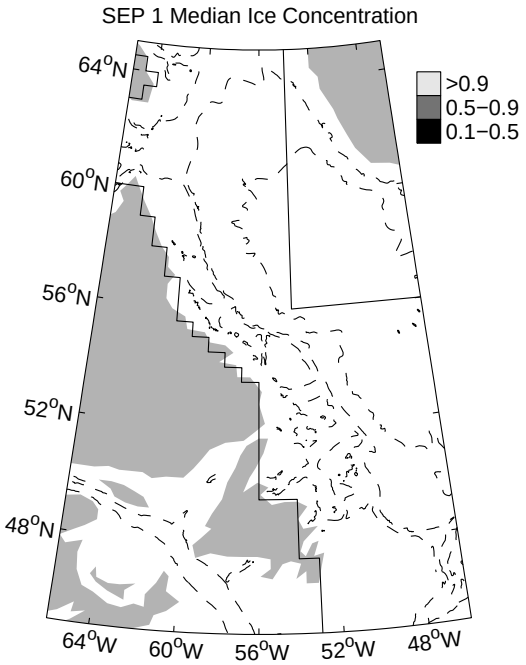
SEP 1 Median Ice Concentration
>0.9
0.5−0.9
0.1−0.5
64°N
60°N
56°N
52°N
48°N
64°W
60°W
56°W
52°W
48°W

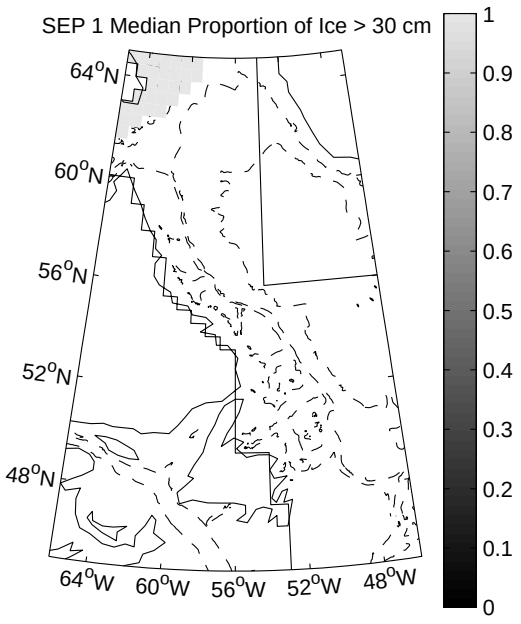
SEP 1 Median Proportion of Ice > 30 cm
1
0.9
0.8
0.7
0.6
0.5
0.4
0.3
0.2
0.1
0
64°N
60°N
56°N
52°N
48°N
64°W
60°W
56°W
52°W
48°W

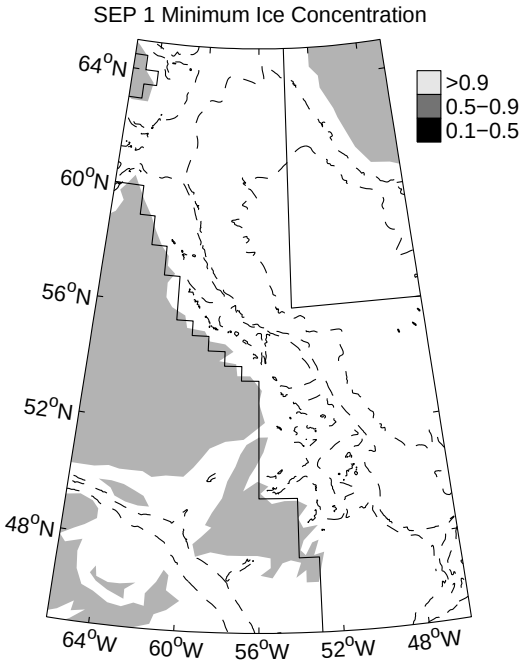
SEP 1 Minimum Ice Concentration
>0.9
0.5−0.9
0.1−0.5
64°N
60°N
56°N
52°N
48°N
64°W
60°W
56°W
52°W
48°W

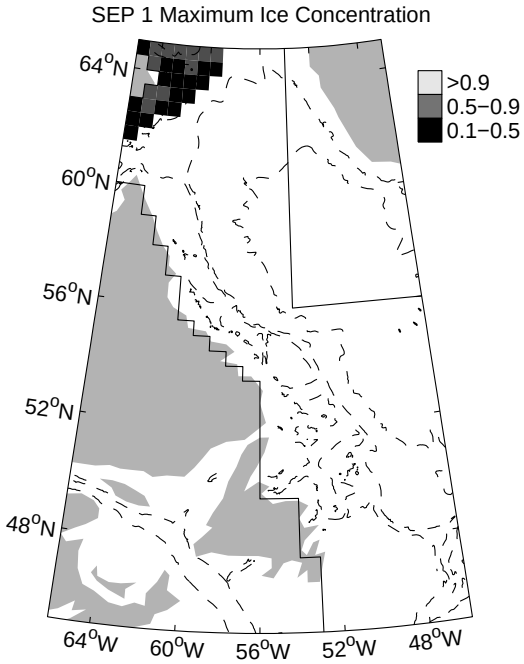
SEP 1 Maximum Ice Concentration
>0.9
0.5−0.9
0.1−0.5
64°N
60°N
56°N
52°N
48°N
64°W
60°W
56°W
52°W
48°W

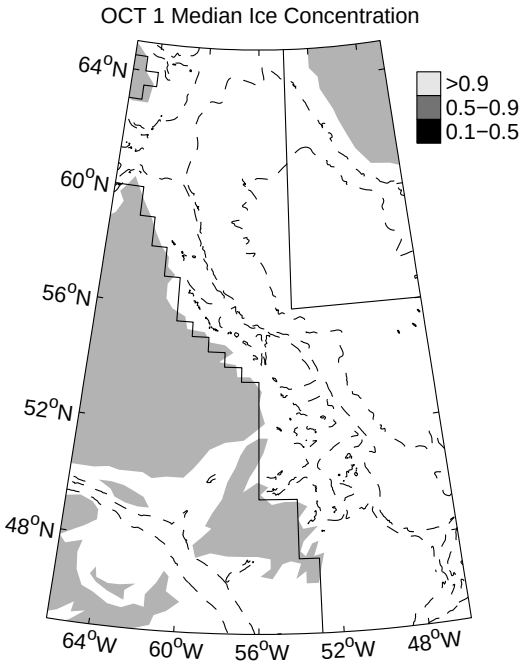
OCT 1 Median Ice Concentration
>0.9
0.5−0.9
0.1−0.5
64°N
60°N
56°N
52°N
48°N
64°W
60°W
56°W
52°W
48°W

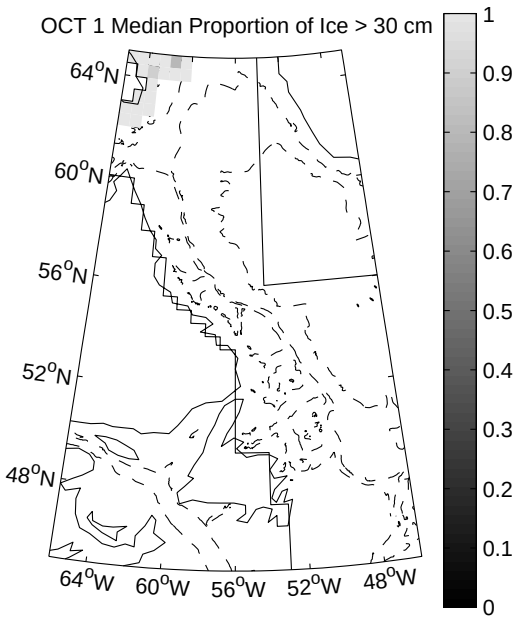
OCT 1 Median Proportion of Ice > 30 cm
1
0.9
0.8
0.7
0.6
0.5
0.4
0.3
0.2
0.1
0
64°N
60°N
56°N
52°N
48°N
64°W
60°W
56°W
52°W
48°W

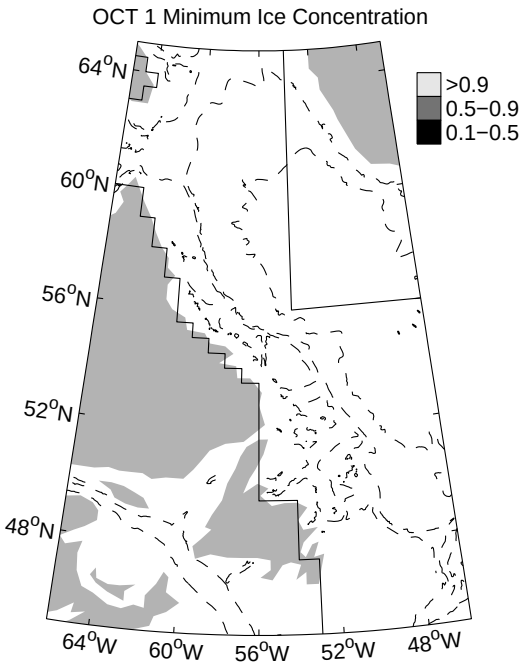
OCT 1 Minimum Ice Concentration
>0.9
0.5−0.9
0.1−0.5
64°N
60°N
56°N
52°N
48°N
64°W
60°W
56°W
52°W
48°W

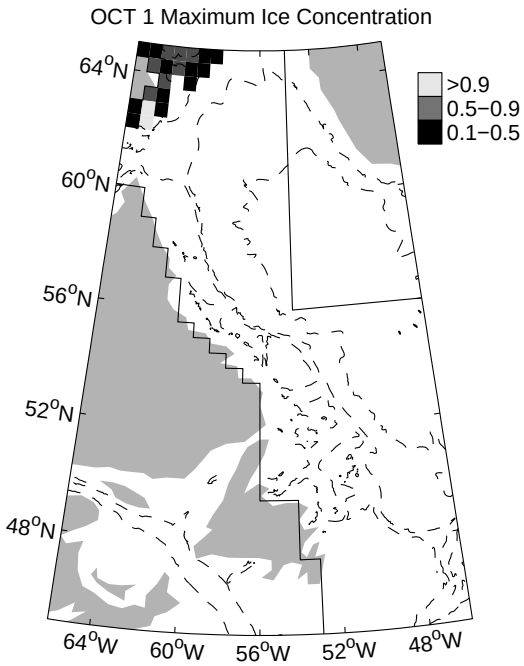
OCT 1 Maximum Ice Concentration
>0.9
0.5−0.9
0.1−0.5
64°N
60°N
56°N
52°N
48°N
64°W
60°W
56°W
52°W
48°W

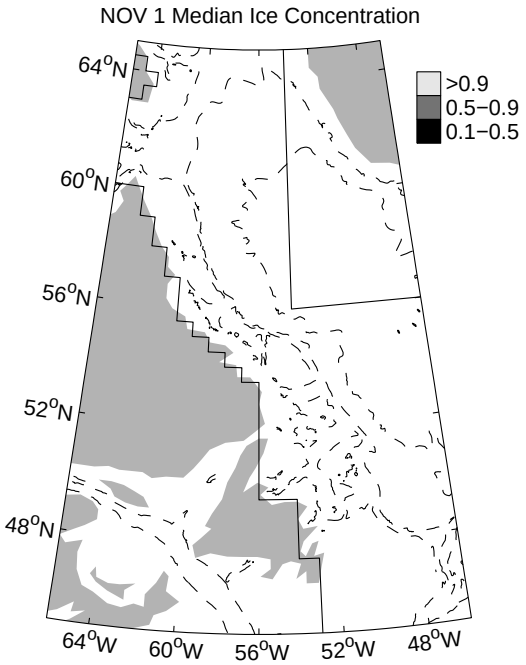
NOV 1 Median Ice Concentration
>0.9
0.5−0.9
0.1−0.5
64°N
60°N
56°N
52°N
48°N
64°W
60°W
56°W
52°W
48°W

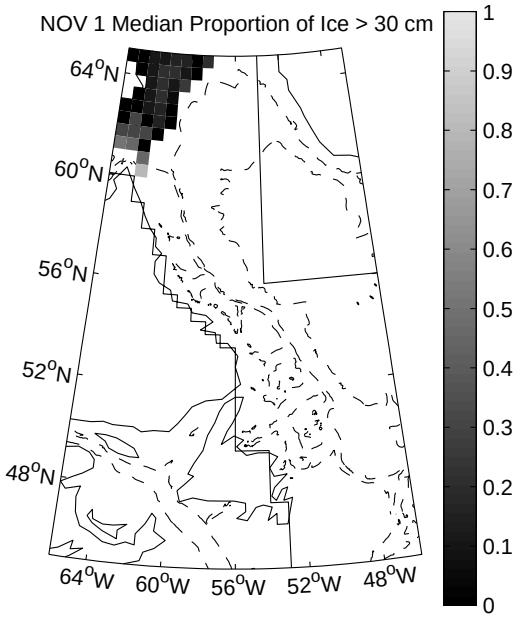
NOV 1 Median Proportion of Ice > 30 cm
1
0.9
0.8
0.7
0.6
0.5
0.4
0.3
0.2
0.1
0
64°N
60°N
56°N
52°N
48°N
64°W
60°W
56°W
52°W
48°W

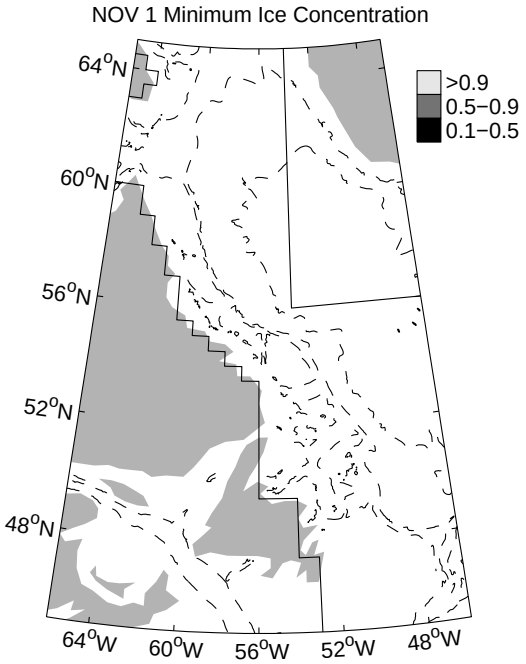
NOV 1 Minimum Ice Concentration
>0.9
0.5−0.9
0.1−0.5
64°N
60°N
56°N
52°N
48°N
64°W
60°W
56°W
52°W
48°W

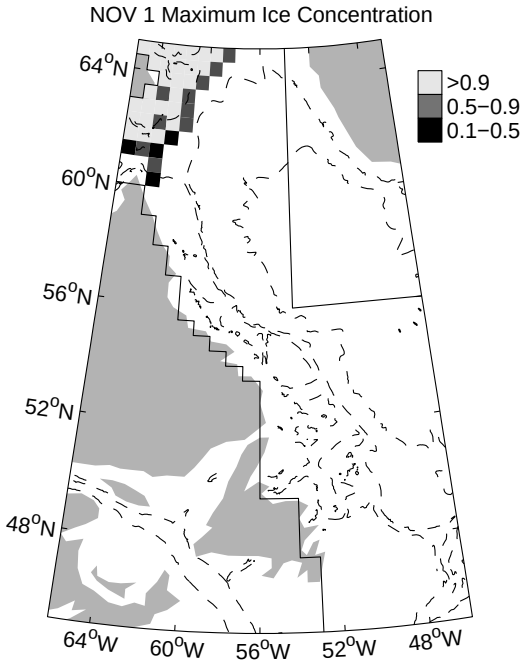
NOV 1 Maximum Ice Concentration
>0.9
0.5−0.9
0.1−0.5
64°N
60°N
56°N
52°N
48°N
64°W
60°W
56°W
52°W
48°W

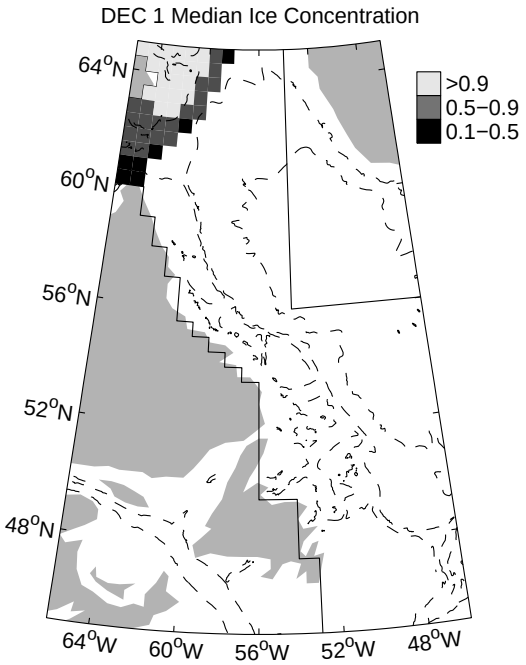
DEC 1 Median Ice Concentration
>0.9
0.5−0.9
0.1−0.5
64°N
60°N
56°N
52°N
48°N
64°W
60°W
56°W
52°W
48°W

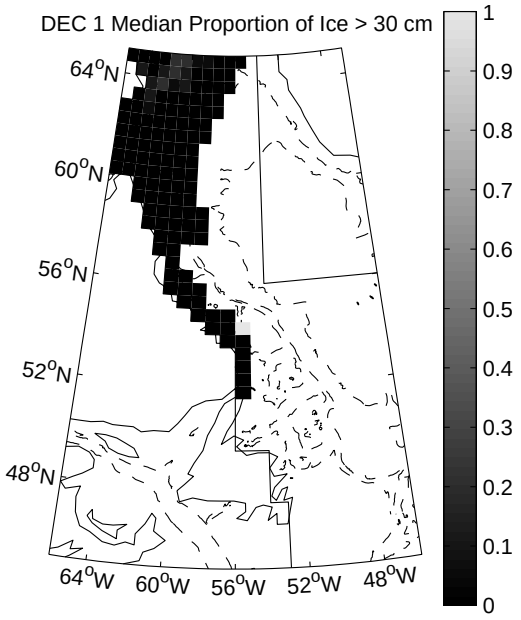
DEC 1 Median Proportion of Ice > 30 cm
1
0.9
0.8
0.7
0.6
0.5
0.4
0.3
0.2
0.1
0
64°N
60°N
56°N
52°N
48°N
64°W
60°W
56°W
52°W
48°W

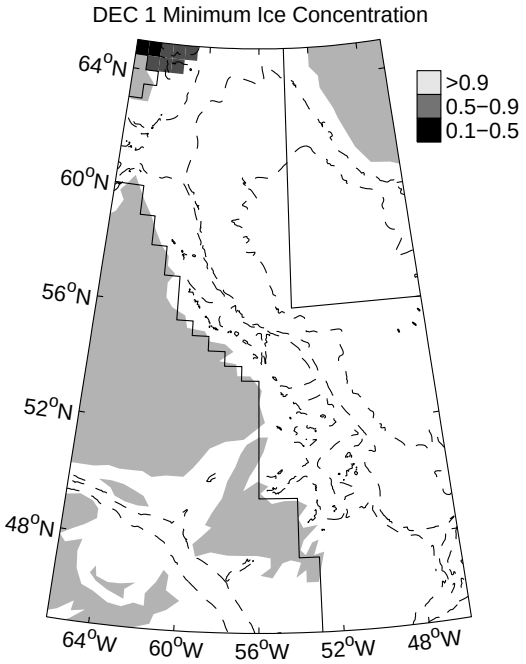
DEC 1 Minimum Ice Concentration
>0.9
0.5−0.9
0.1−0.5
64°N
60°N
56°N
52°N
48°N
64°W
60°W
56°W
52°W
48°W

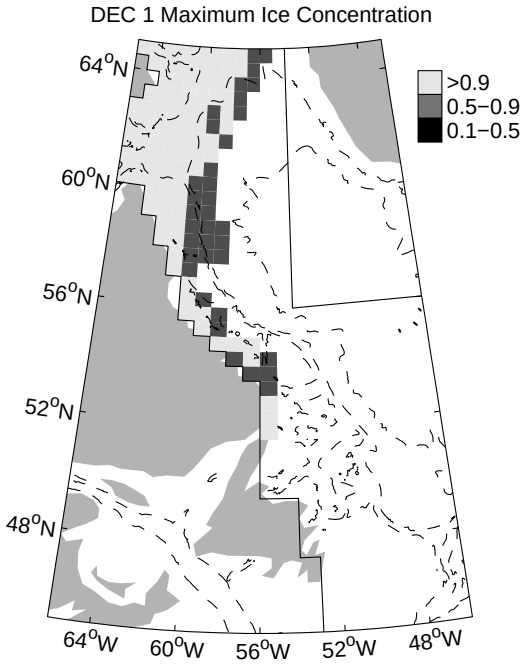
DEC 1 Maximum Ice Concentration
>0.9
0.5−0.9
0.1−0.5
64°N
60°N
56°N
52°N
48°N
64°W
60°W
56°W
52°W
48°W

APPENDIX B

Correlations (r) of monthly negative air temperature at Iqaluit, Cartwright and St. John's with sea ice extent in latitude bands from 45°N to 65°N

Each figure shows the correlation of mean negative air temperature for the given month with ice extent at the start of all other months.

The vertical dashed line indicates zero lag in time, i.e. correlation of air temperature and ice extent for the same month. The horizontal dashed line indicates the latitude of the given air temperature station.

Iqaluit

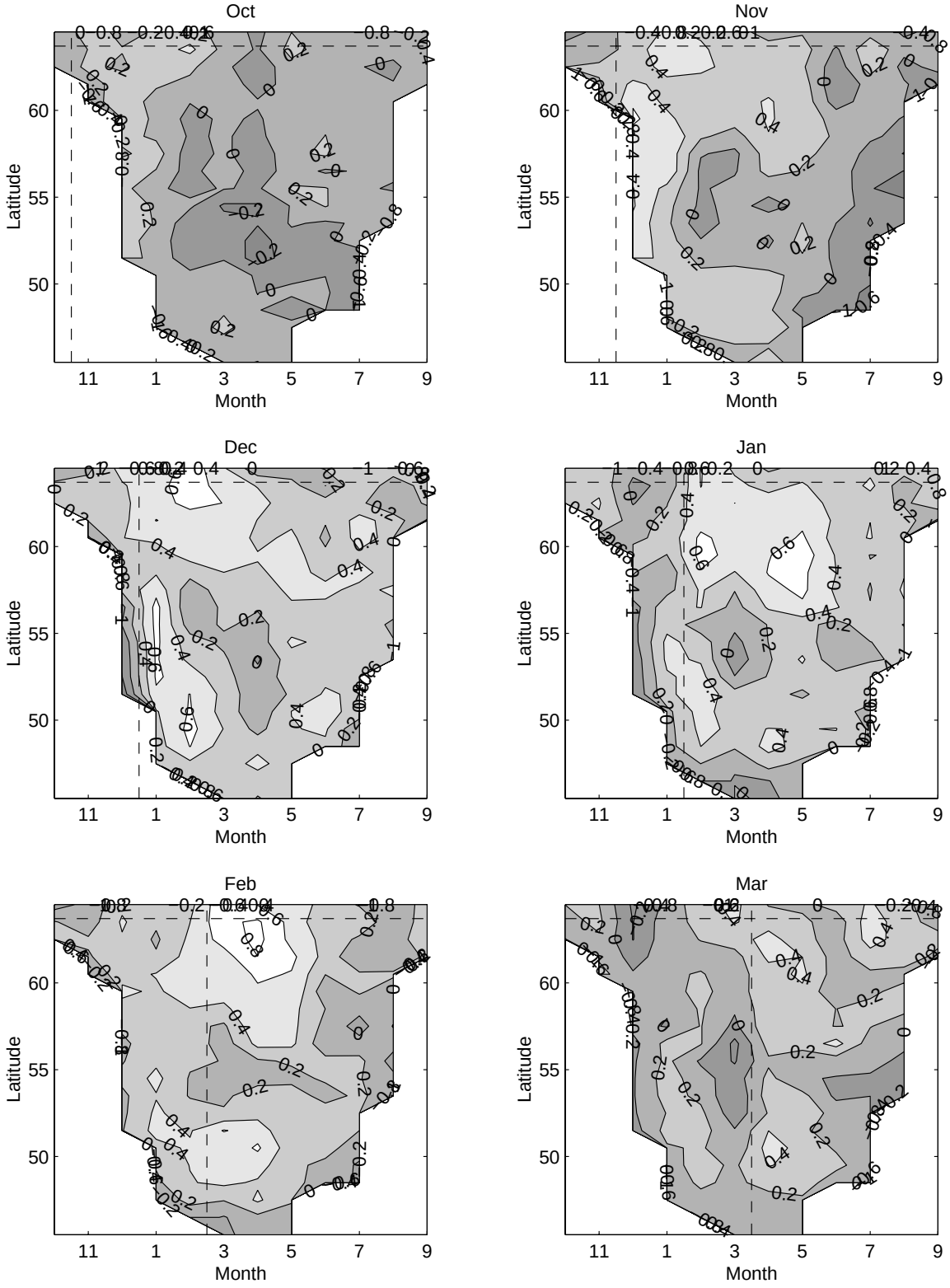

Iqaluit

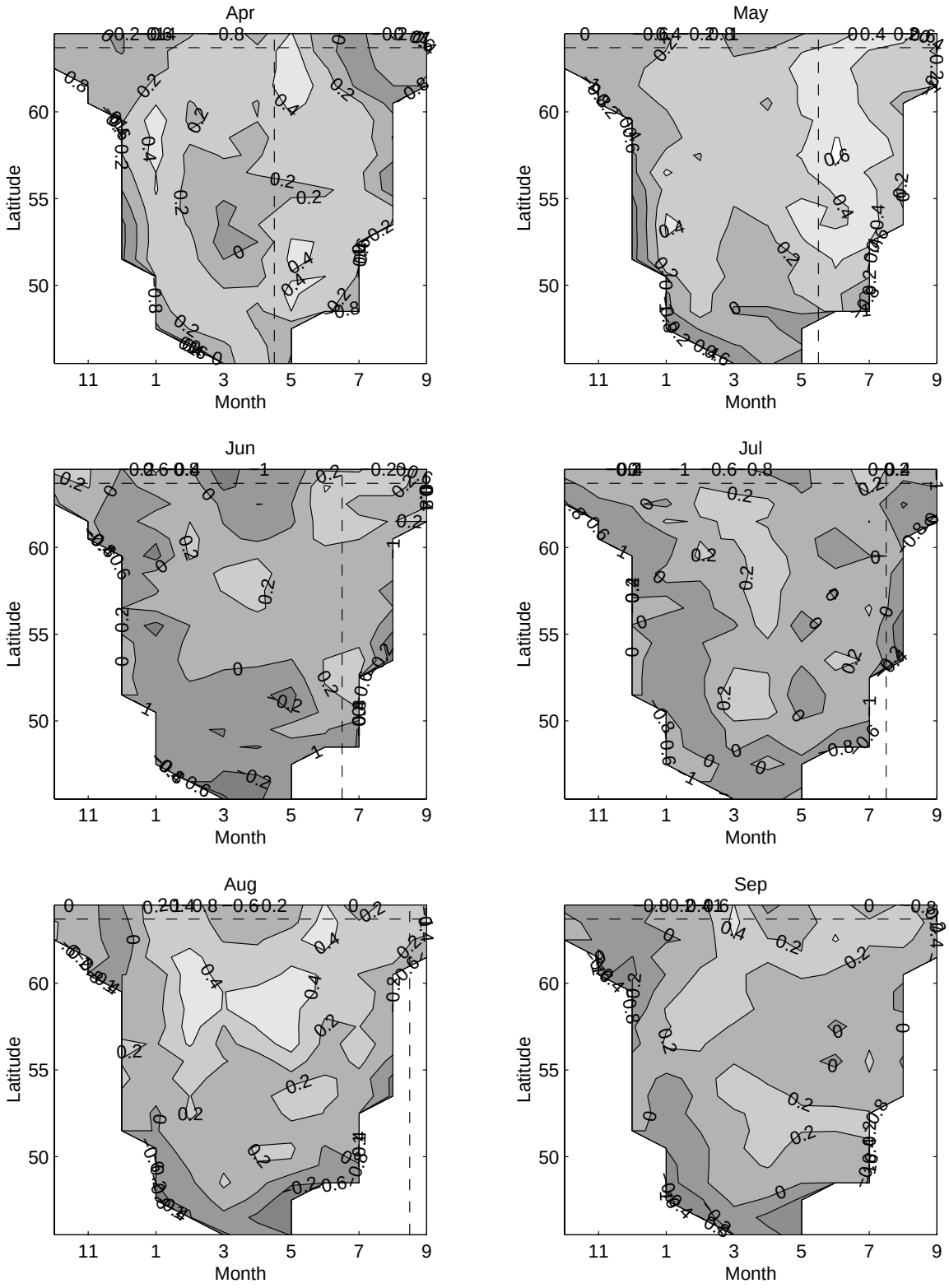

Cartwright

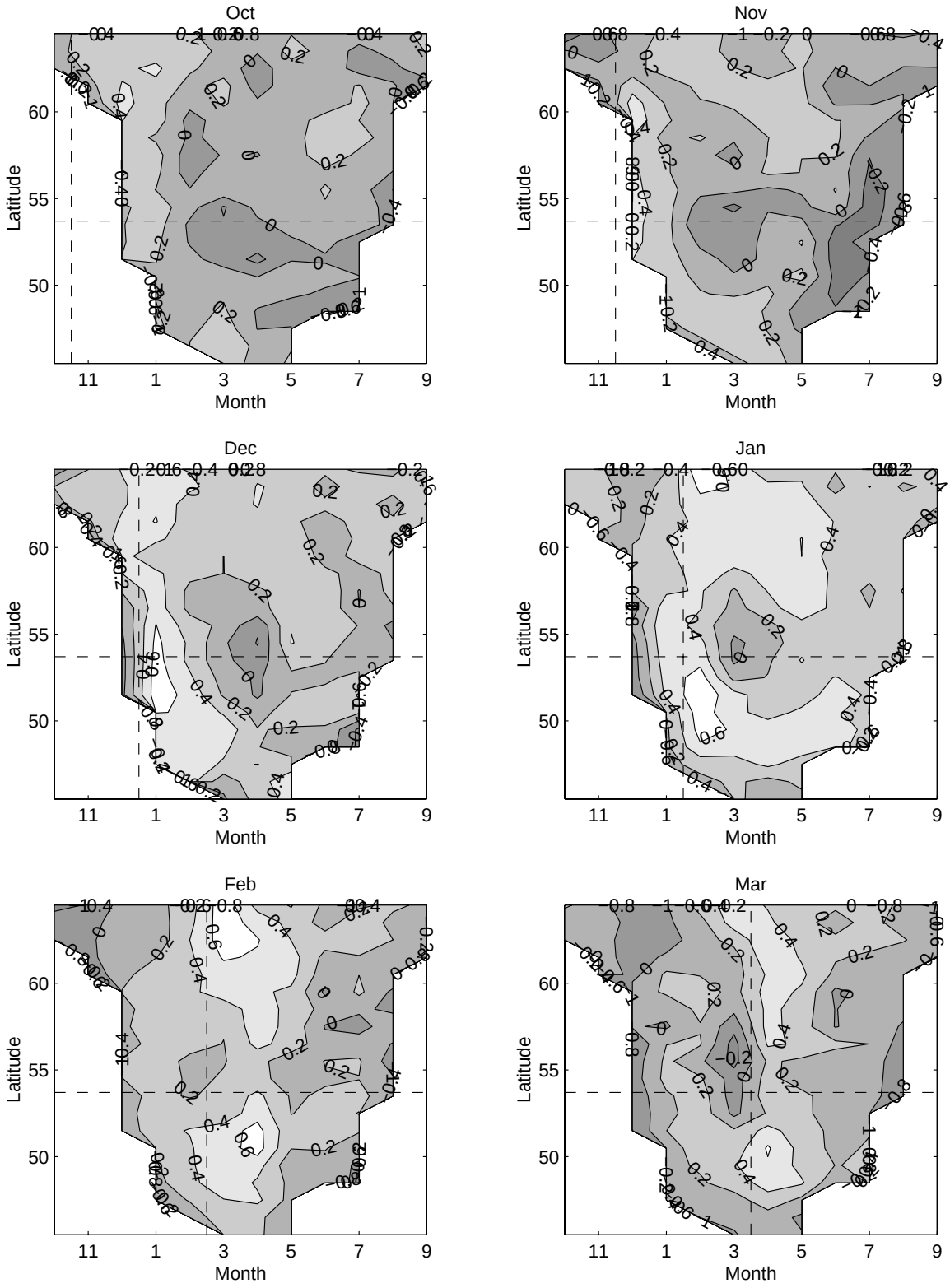

Cartwright

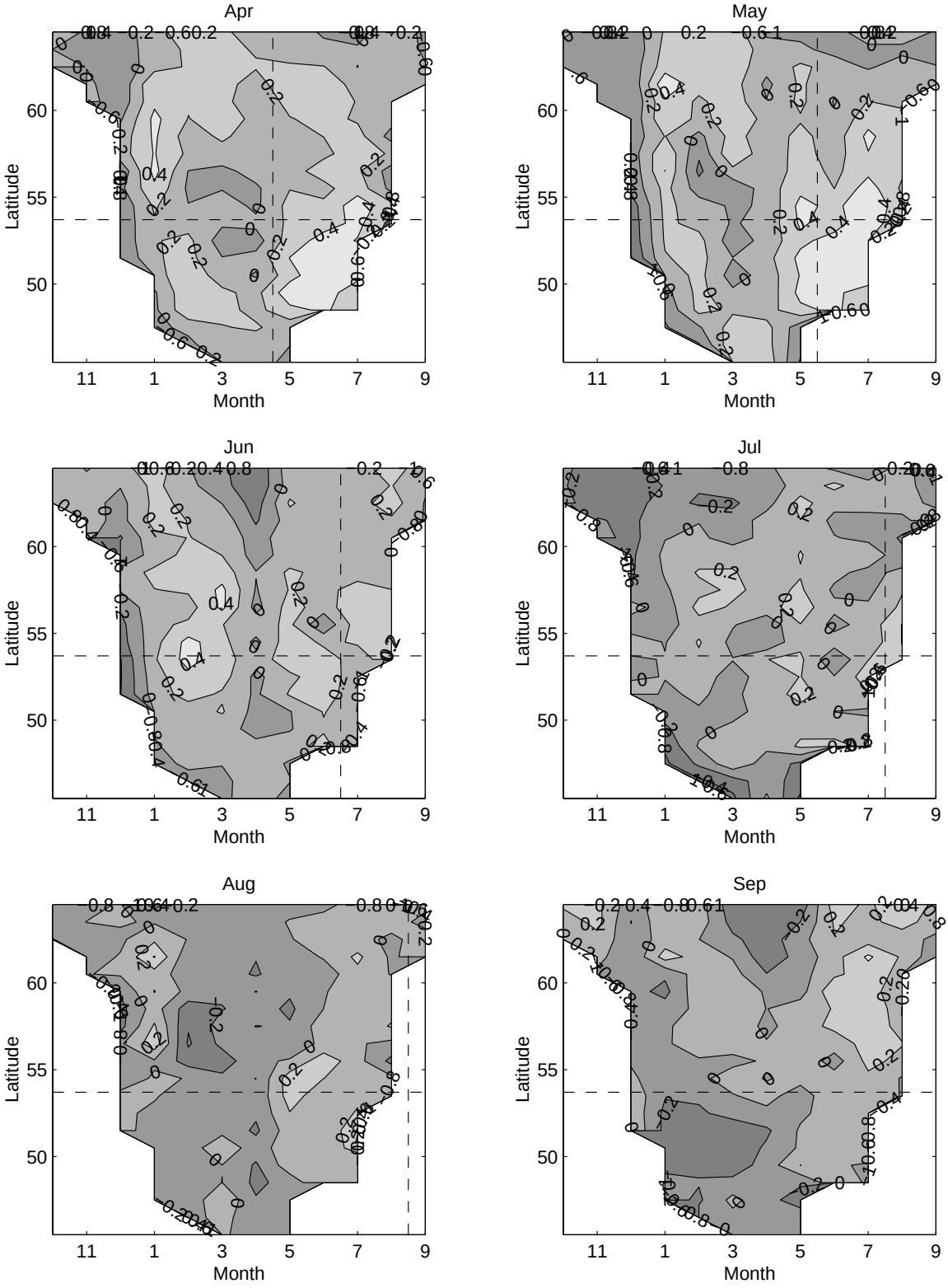

St. John's

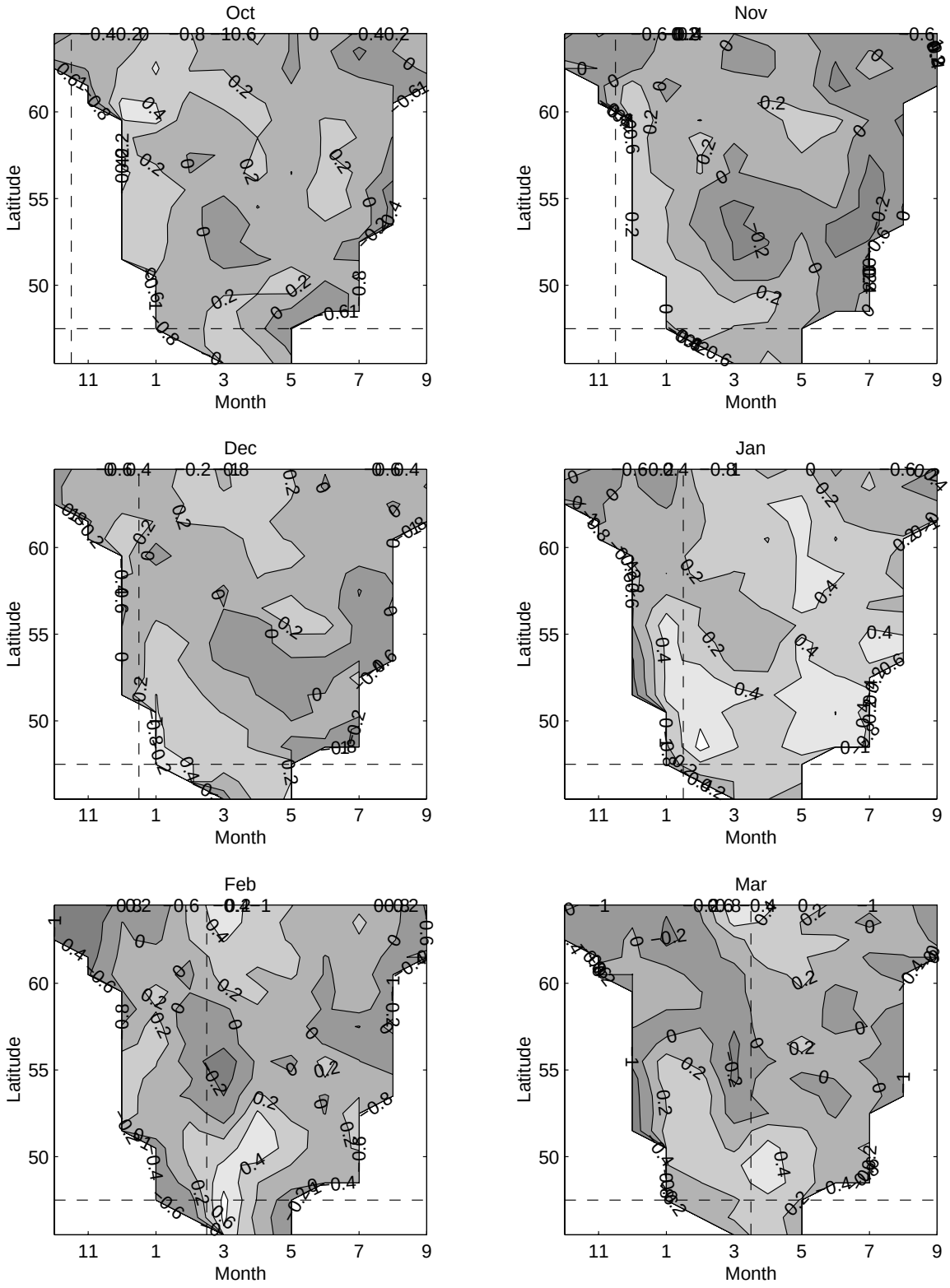

St. John's

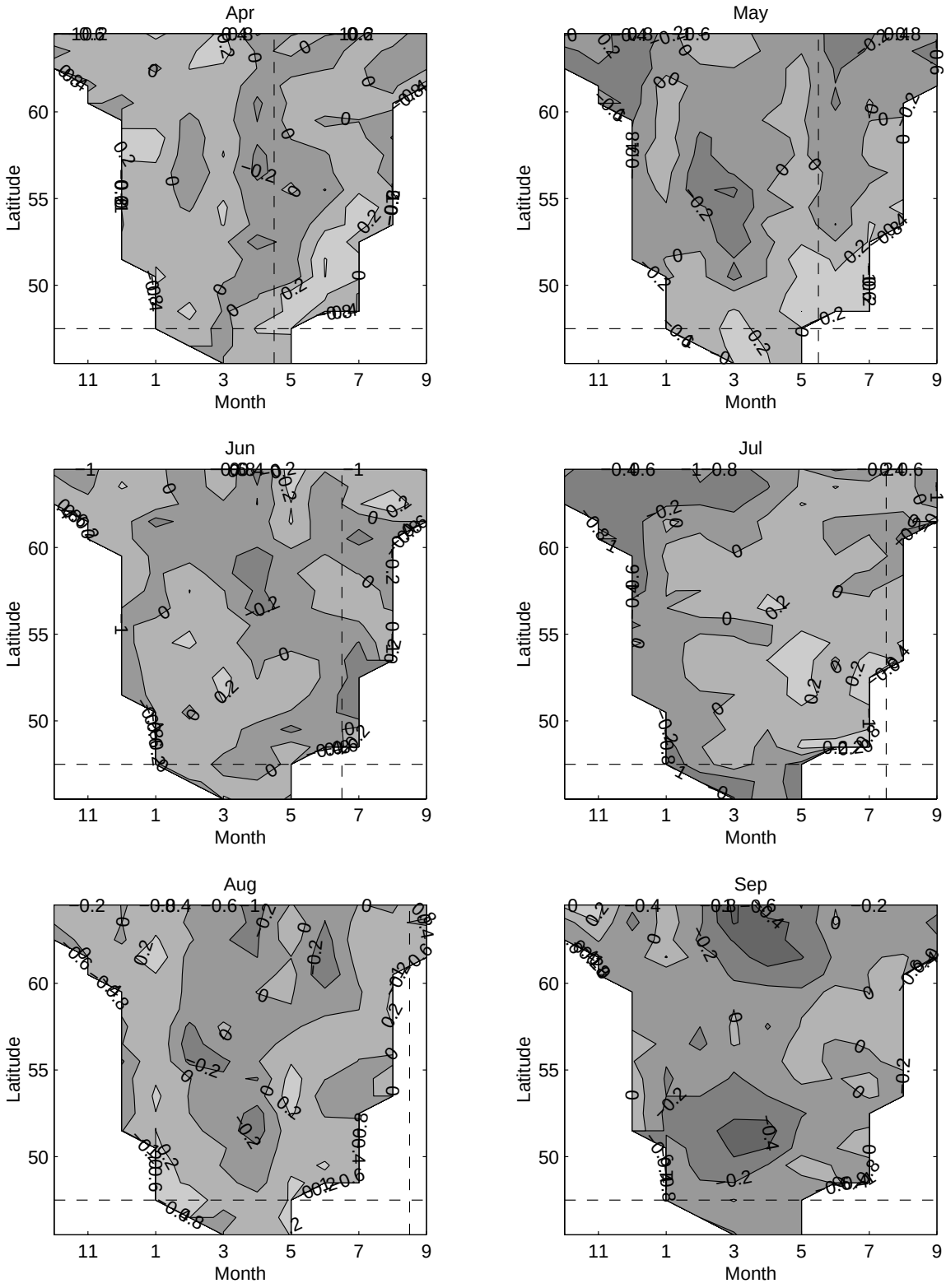

APPENDIX C

Winter NCEP sea level pressure maps (Dec-Feb)

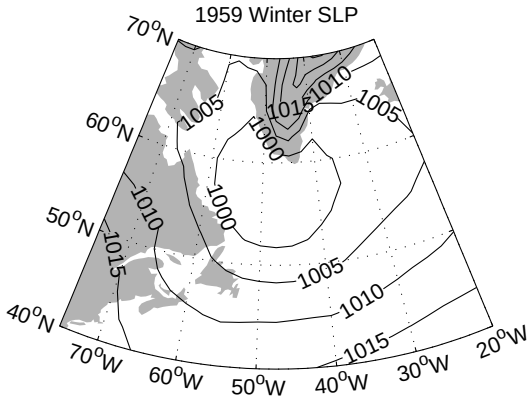
1959 Winter SLP
70°N
60°N
50°N
40°N
70°W
60°W
50°W
40°W
30°W
20°W
1005
1010
1015
1000
1010
1015
1005
1000
1005
1010
1015

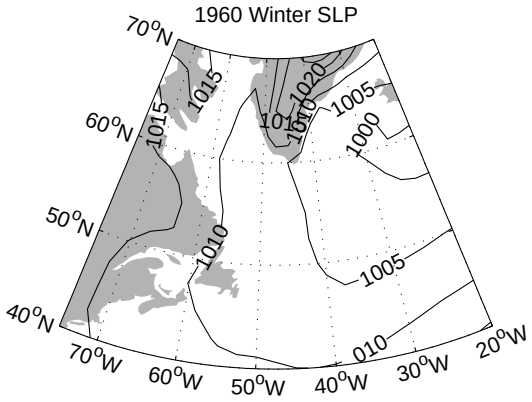
1960 Winter SLP
70°N
60°N
50°N
40°N
70°W
60°W
50°W
40°W
30°W
20°W
1015
1020
1005
1000
1010
1005
010

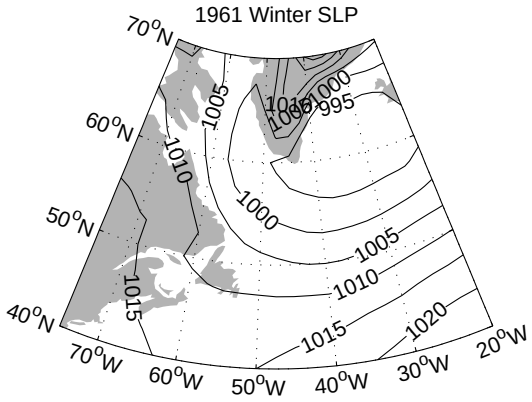
1961 Winter SLP
70°N
60°N
50°N
40°N
70°W
60°W
50°W
40°W
30°W
20°W
1005
1000
995
1010
1000
1005
1010
1015
1015
1020

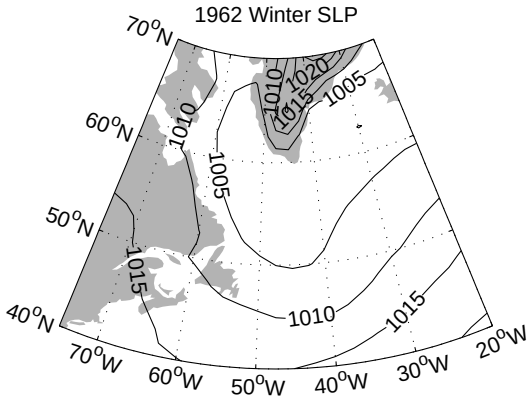
1962 Winter SLP
70°N
60°N
50°N
40°N
70°W
60°W
50°W
40°W
30°W
20°W
1010
1020
1015
1005
1010
1005
1015
1010
1015

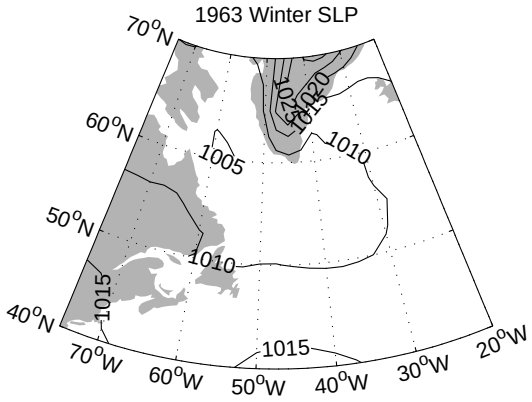
1963 Winter SLP
70°N
60°N
50°N
40°N
70°W
60°W
50°W
40°W
30°W
20°W
1020
1015
1005
1010
1010
1015
1015

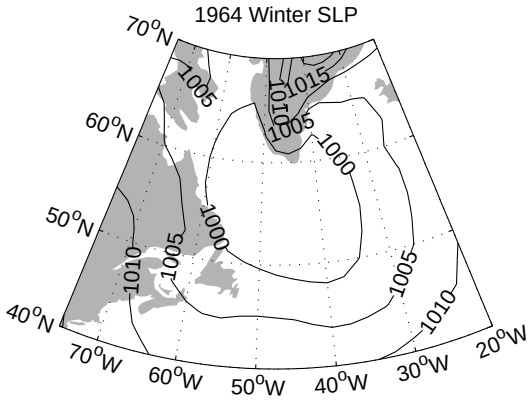
1964 Winter SLP
70°N
60°N
50°N
40°N
70°W
60°W
50°W
40°W
30°W
20°W
1005
1015
1010
1005
1000
1010
1005
1000
1005
1010

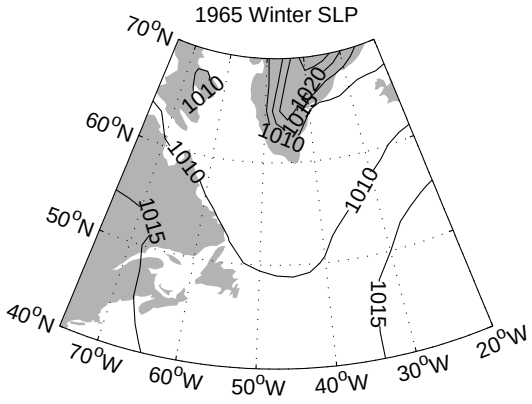
1965 Winter SLP
70°N
60°N
50°N
40°N
70°W
60°W
50°W
40°W
30°W
20°W
1010
1015
1020
1010
1010
1010
1015
1015

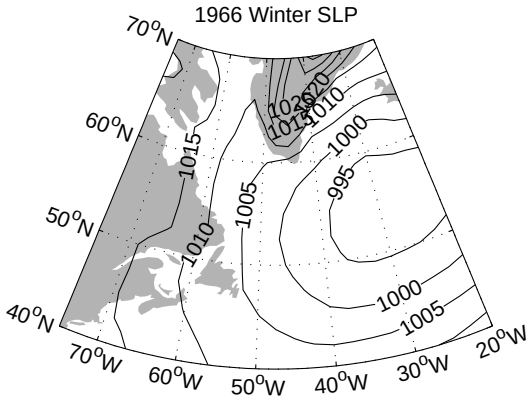
1966 Winter SLP
70°N
60°N
50°N
40°N
70°W
60°W
50°W
40°W
30°W
20°W
1020
1015
1010
1015
1000
995
1005
1010
1000
1005

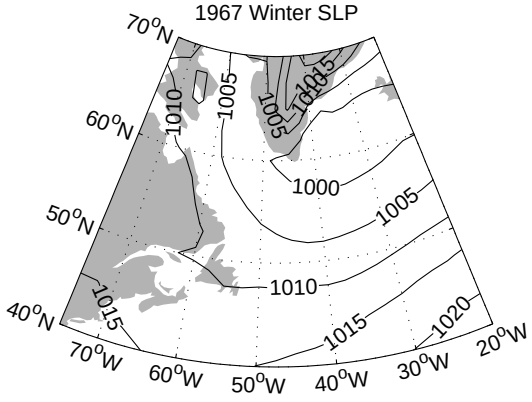
1967 Winter SLP
70°N
60°N
50°N
40°N
70°W
60°W
50°W
40°W
30°W
20°W
1010
1005
1015
1005
1000
1005
1010
1015
1015
1020

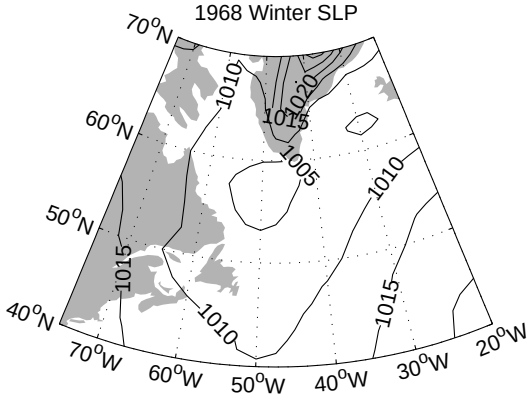
1968 Winter SLP
70°N
60°N
50°N
40°N
70°W
60°W
50°W
40°W
30°W
20°W
1010
1020
1015
1005
1010
1015
1015
1010

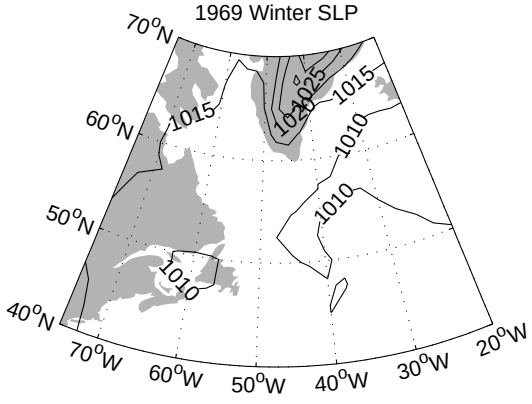
1969 Winter SLP
70°N
60°N
50°N
40°N
70°W
60°W
50°W
40°W
30°W
20°W
1025
1020
1015
1015
1010
1010
1010

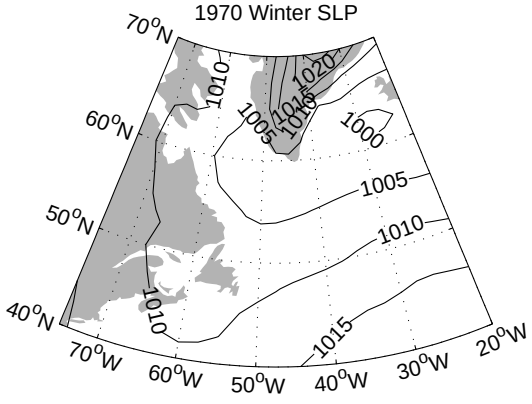
1970 Winter SLP
70°N
60°N
50°N
40°N
70°W
60°W
50°W
40°W
30°W
20°W
1010
1020
1015
1005
1015
1000
1005
1010
1010
1015

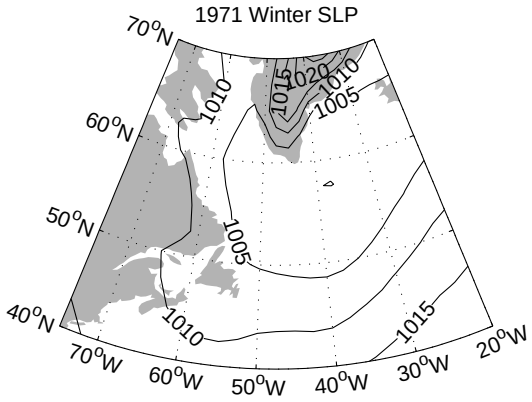
1971 Winter SLP
70°N
60°N
50°N
40°N
70°W
60°W
50°W
40°W
30°W
20°W
1010
1015
1020
1010
1005
1005
1010
1015

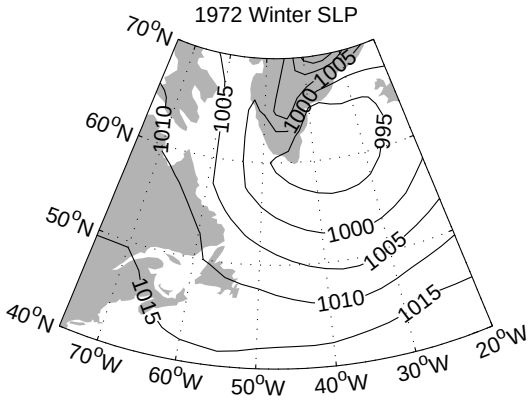
1972 Winter SLP
70°N
60°N
50°N
40°N
70°W
60°W
50°W
40°W
30°W
20°W
1010
1005
1000
1005
995
1000
1005
1010
1015
1015

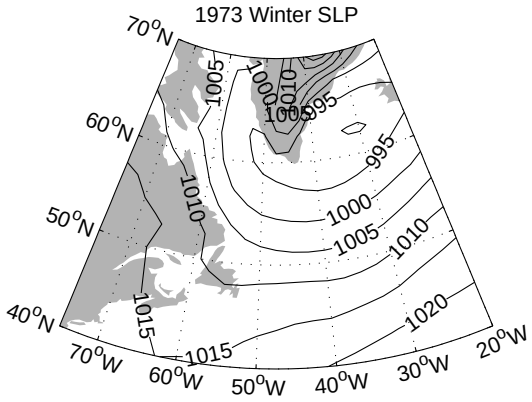
1973 Winter SLP
70°N
60°N
50°N
40°N
70°W
60°W
50°W
40°W
30°W
20°W
1005
1000
1010
1005
995
995
1000
1005
1010
1020
1010
1015
1015

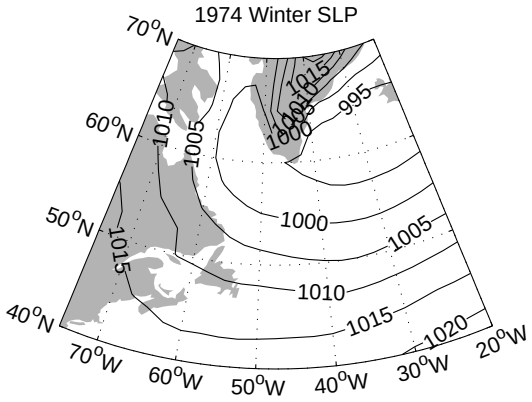
1974 Winter SLP
70°N
60°N
50°N
40°N
70°W
60°W
50°W
40°W
30°W
20°W
1010
1005
1015
1000
995
1000
1005
1010
1015
1020
1015

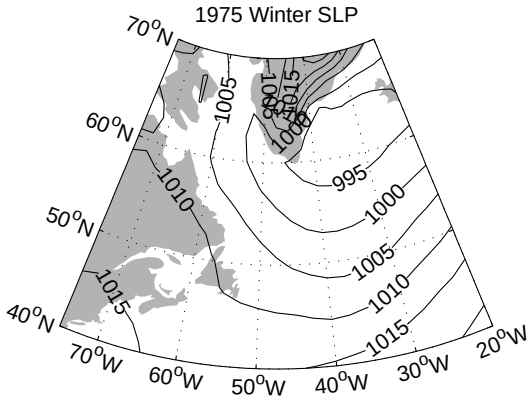
1975 Winter SLP
70°N
60°N
50°N
40°N
70°W
60°W
50°W
40°W
30°W
20°W
1005
1000
1010
995
1000
1005
1010
1015
1015

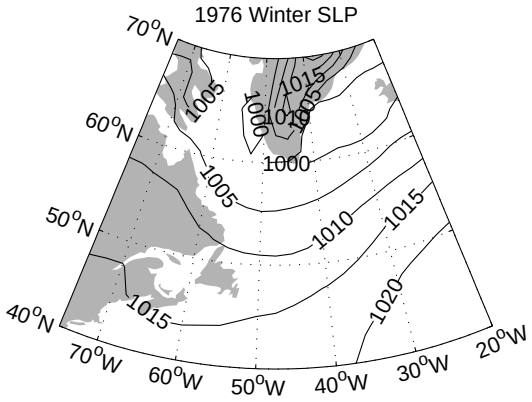
1976 Winter SLP
70°N
60°N
50°N
40°N
70°W
60°W
50°W
40°W
30°W
20°W
1005
1015
1000
1000
1005
1010
1015
1020
1015

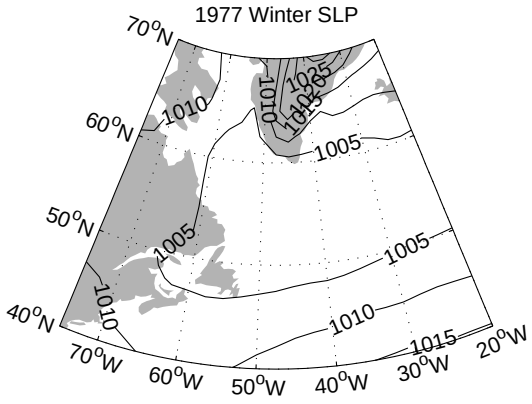
1977 Winter SLP
70°N
60°N
50°N
40°N
70°W
60°W
50°W
40°W
30°W
20°W
1010
1005
1015
1025

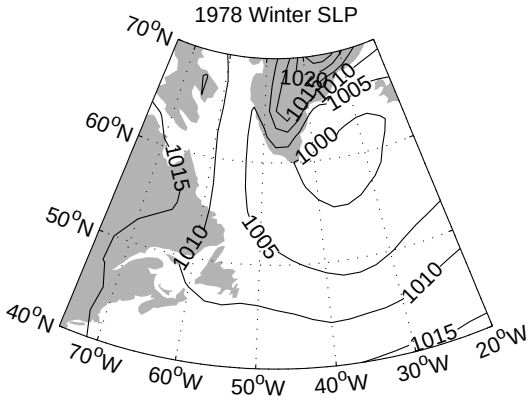
1978 Winter SLP
70°N
60°N
50°N
40°N
70°W
60°W
50°W
40°W
30°W
20°W
1020
1015
1010
1005
1000
1015
1010
1005
1010
1015

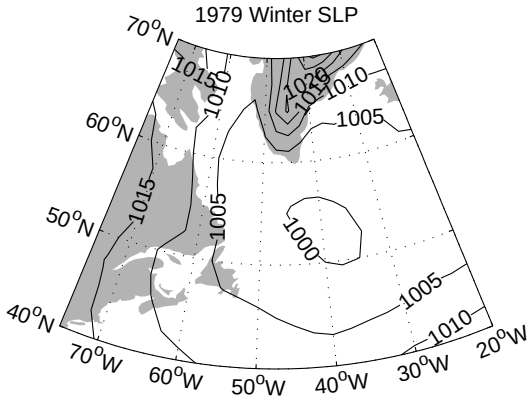
1979 Winter SLP
70°N
60°N
50°N
40°N
70°W
60°W
50°W
40°W
30°W
20°W
1015
1010
1020
1010
1005
1015
1005
1000
1005
1010

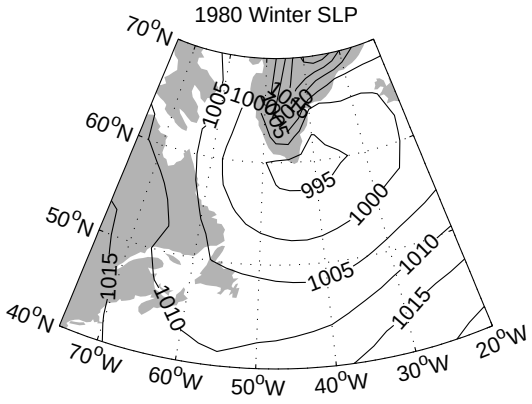
1980 Winter SLP
70°N
60°N
50°N
40°N
70°W
60°W
50°W
40°W
30°W
20°W
1005
1000
1010
995
1000
1015
1010
1005
1010
1015

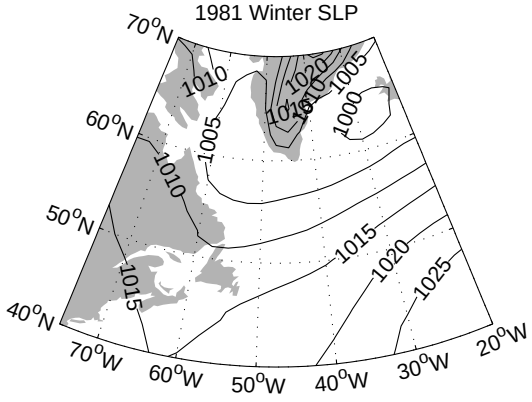
1981 Winter SLP
70°N
60°N
50°N
40°N
70°W
60°W
50°W
40°W
30°W
20°W
1010
1020
1005
1000
1005
1010
1015
1015
1020
1025

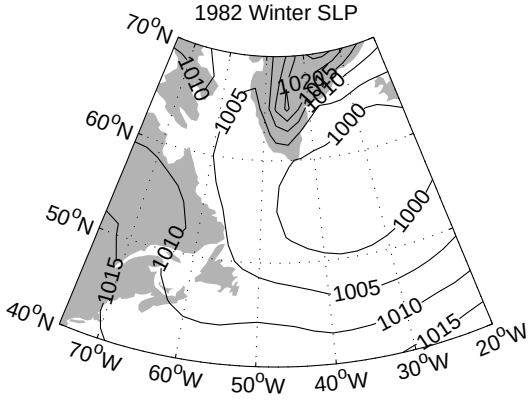
1982 Winter SLP
70°N
60°N
50°N
40°N
70°W
60°W
50°W
40°W
30°W
20°W
1010
1005
1020
1000
1000
1010
1015
1005
1010
1015

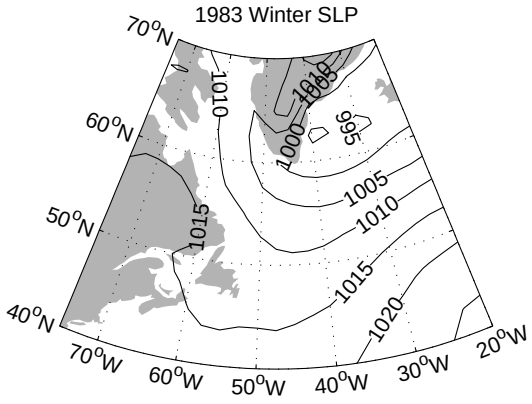
1983 Winter SLP
70°N
60°N
50°N
40°N
70°W
60°W
50°W
40°W
30°W
20°W
1010
1005
1000
995
1015
1020

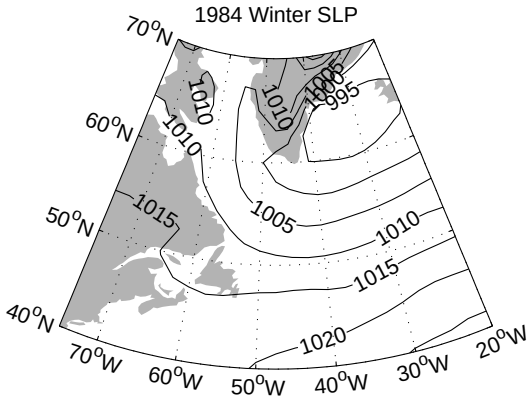
1984 Winter SLP
70°N
60°N
50°N
40°N
70°W
60°W
50°W
40°W
30°W
20°W
1010
1005
995
1015
1020

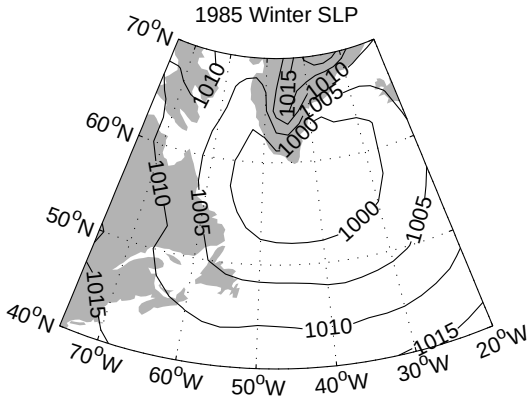
1985 Winter SLP
70°N
60°N
50°N
40°N
70°W
60°W
50°W
40°W
30°W
20°W
1010
1015
1005
1000
1020

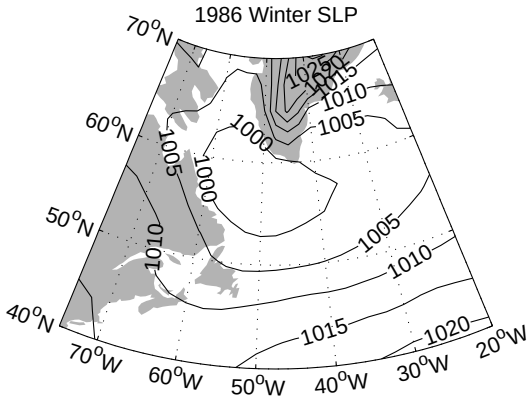
1986 Winter SLP
70°N
60°N
50°N
40°N
70°W
60°W
50°W
40°W
30°W
20°W
1025
1015
1010
1005
1000
1020

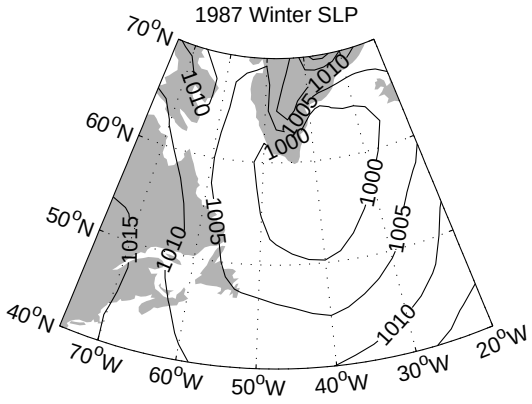
1987 Winter SLP
70°N
60°N
50°N
40°N
70°W
60°W
50°W
40°W
30°W
20°W
1010
1005
1000
1015

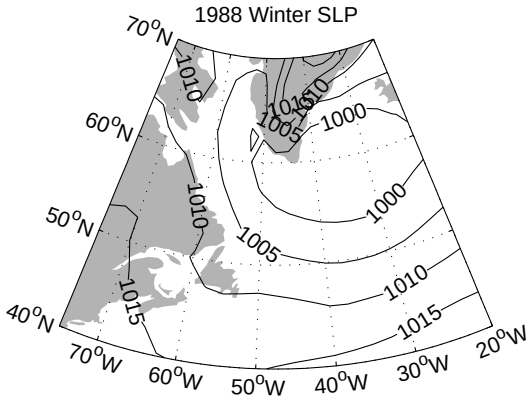
1988 Winter SLP
70°N
60°N
50°N
40°N
70°W
60°W
50°W
40°W
30°W
20°W
1010
1005
1000
1015

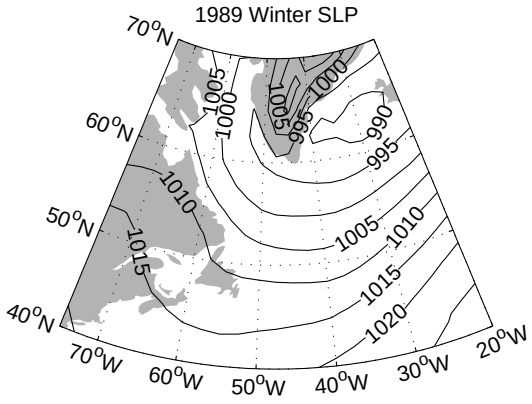
1989 Winter SLP
70°N
60°N
50°N
40°N
70°W
60°W
50°W
40°W
30°W
20°W
1000
1005
995
990
1010
1015
1020

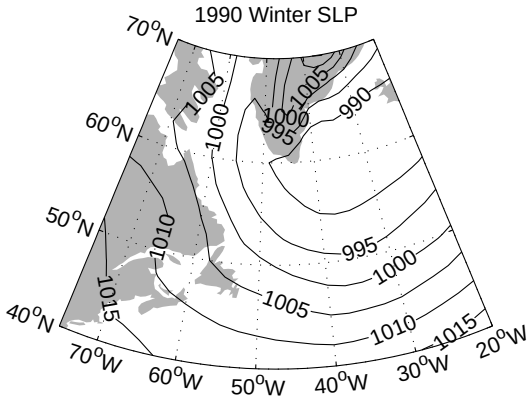
1990 Winter SLP
70°N
60°N
50°N
40°N
70°W
60°W
50°W
40°W
30°W
20°W
1005
1000
995
990
1010
1015

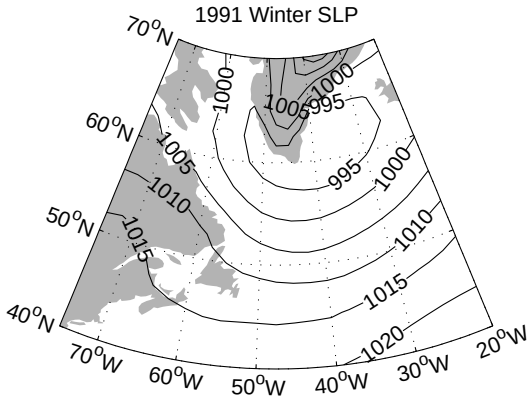
1991 Winter SLP
70°N
60°N
50°N
40°N
70°W
60°W
50°W
40°W
30°W
20°W
1000
1005
995
1010
1015
1020

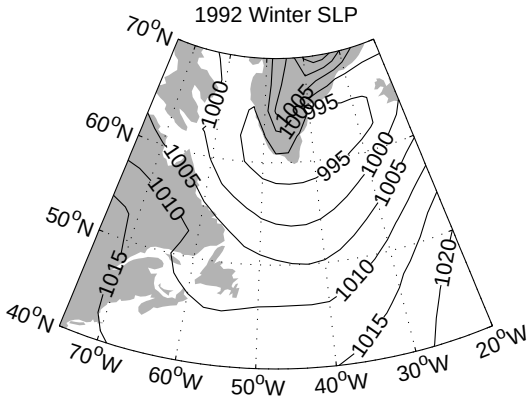
1992 Winter SLP
70°N
60°N
50°N
40°N
70°W
60°W
50°W
40°W
30°W
20°W
1000
1005
995
1010
1015
1020

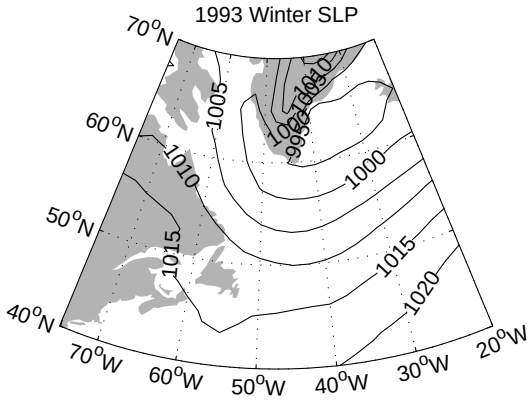
1993 Winter SLP
70°N
60°N
50°N
40°N
70°W
60°W
50°W
40°W
30°W
20°W
1005
1000
995
1010
1015
1020

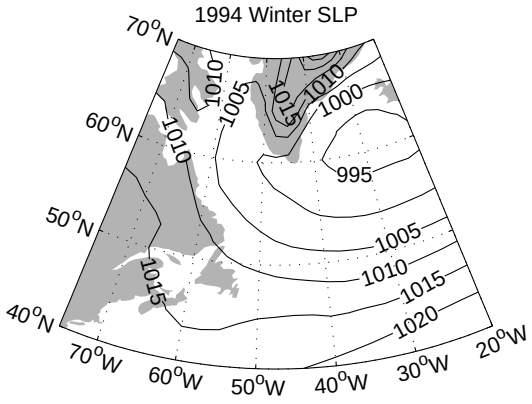
1994 Winter SLP
70°N
60°N
50°N
40°N
70°W
60°W
50°W
40°W
30°W
20°W
1010
1005
1000
995
1015
1020

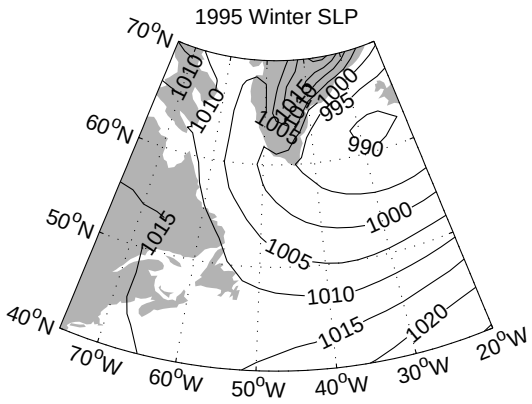
1995 Winter SLP
70°N
60°N
50°N
40°N
70°W
60°W
50°W
40°W
30°W
20°W
1010
1010
1015
1015
1000
995
990
1000
1005
1010
1015
1020

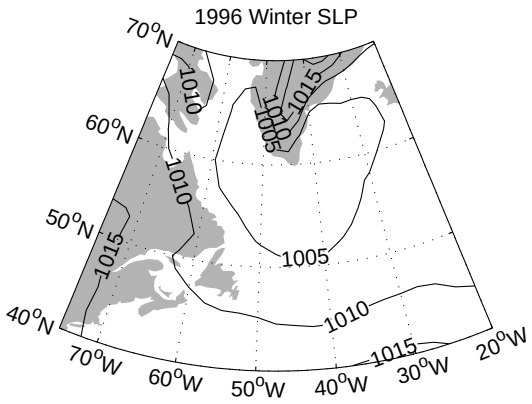
1996 Winter SLP
70°N
60°N
50°N
40°N
70°W
60°W
50°W
40°W
30°W
20°W
1010
1015
1005
1010
1015
1005
1010
1015

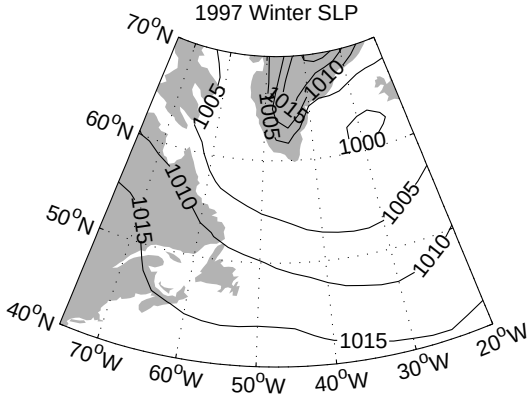
1997 Winter SLP
70°N
60°N
50°N
40°N
70°W
60°W
50°W
40°W
30°W
20°W
1005
1005
1010
1010
1000
1005
1010
1015
1015

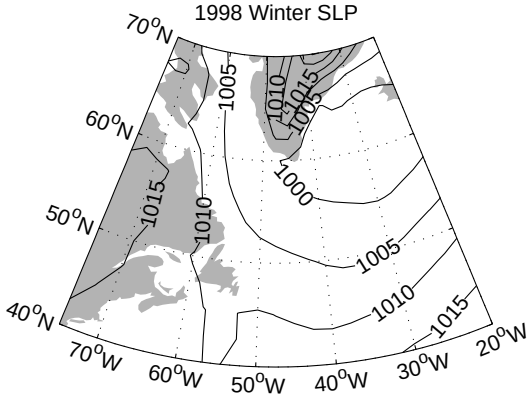
1998 Winter SLP
70°N
60°N
50°N
40°N
70°W
60°W
50°W
40°W
30°W
20°W
1005
1010
1015
1005
1000
1015
1010
1005
1010
1015